JOURNAL OF PETROLOGY | VOLUME 39 | NUMBER 8 | PAGES 1493–1526 | 1998

Migrating Cretaceous–Eocene Magmatism in the Serra do Mar Alkaline Province, SE Brazil: Melts from the Deflected Trindade Mantle Plume?

R. N. THOMPSON[1]*, S. A. GIBSON[2], J. G. MITCHELL[3], A. P. DICKIN[4], O. H. LEONARDOS[5], J. A. BROD[1,5] AND J. C. GREENWOOD[2]

[1]DEPARTMENT OF GEOLOGICAL SCIENCES, UNIVERSITY OF DURHAM, SOUTH ROAD, DURHAM DH1 3LE, UK

[2]DEPARTMENT OF EARTH SCIENCES, UNIVERSITY OF CAMBRIDGE, DOWNING STREET, CAMBRIDGE CB2 3EQ, UK

[3]DEPARTMENT OF PHYSICS, THE UNIVERSITY, NEWCASTLE UPON TYNE NE1 7RU, UK

[4]DEPARTMENT OF GEOLOGY, McMASTER UNIVERSITY, 1280 MAIN STREET WEST, HAMILTON, ONT., CANADA L8S 4M1

[5]DEPARTMENTO DE GEOQUIMÍCA E RECURSOS MINERAIS, INSTITUTO DE GEOCIÊNCIAS, UNIVERSIDADE DE BRASÍLIA, 70910 BRASÍLIA DF, BRAZIL

RECEIVED JULY 30, 1997; REVISED TYPESCRIPT ACCEPTED MARCH 3, 1998

*The Serra do Mar province extends for ~500 km as plutonic complexes, some with volcanic remnants, and dyke swarms along coastal SE Brazil. The igneous rocks are emplaced into metamorphics of the Brasiliano (Pan-African) Ribeira mobile belt, which abuts the southern margin of the Archaean São Francisco craton. Syenites and phonolites dominate most complexes but mafic–ultramafic dykes (MgO <16·4%) are also widespread, together with sparse mafic lavas. The mafic rocks are alkali basalts, basanites and melanephelinites, with rare leucitites and minettes (*s.l.*). Major and trace elements of all but a few of the strongly potassic rock types are indistinguishable from ocean-island basaltic (OIB,* s.l.*) magmatism. Isotopically (Sr–Nd), the Serra do Mar suite overlaps the field for OIB (ε_{Nd} up to +2·7) and aseismic ridges, especially Walvis. In general, the most potassic compositions have the lowest ε_{Nd} values (–1·4 to –3·3). We consider the most plausible source for Serra do Mar mafic magmas to be predominantly sub-lithospheric convecting mantle, with sporadic input from lithospheric metasomites. Additionally, the two most Mg-rich dykes have high $^{87}Sr/^{86}Sr_i$ (>0·707), despite ε_{Nd} in the same range as nearby mafic dykes. We attribute this to upper-crust contamination during turbulent emplacement of very hot, low-viscosity magma batches. New K/Ar dates, together with a detailed assessment of published ages, show that the initiation of Serra do Mar magmatism migrated progressively ~500 km ESE, from Poços de Caldas to Cabo Frio, between ~80 and 55 Ma. It is inferred that the Trindade mantle plume impacted at ~85 Ma beneath interior SE Brazil where the lithosphere was too thick (>150 km), except very locally, to permit dry decompression melting and basaltic (*s.l.*) magma genesis. Instead, strongly alkalic, potassic, lithosphere-source magmatism (including diamondiferous kimberlites) broke out penecontemporaneously over a region of ~600 km radius. Between ~85 and 80 Ma it is suggested that the starting-plume head expanded rapidly beneath the thick continental lithospheric lid. This caused regional kilometre-scale uplift and erosion (evidenced by published apatite fission-track data) for 1200 km to the south, together with strongly alkaline magmatism at Lages, southern Brazil, a site of localized rifting. After ~80 Ma, as the plume tail moved ESE beneath the Archaean São Francisco craton, its magmatic signal at the surface was 'switched off' by the thick (200–250 km) cratonic lithosphere. Nevertheless, hot plume-tail mantle 'leaked' progressively southward, until it encountered strongly thinned lithosphere beneath SE coastal Brazil, along the passive margin of the South American plate, where decompression melting generated the predominant OIB-like component of the Serra do Mar magmatism. After 55 Ma this*

*Corresponding author. e-mail: r.n.thompson@durham.ac.uk

magmatism transferred NE from Cabo Frio to the Abrolhos Platform (52 Ma), the landward terminus of the seamount chain leading to the islands of Trindade and Martin Vaz in the South Atlantic.

KEY WORDS: *basic magmas; SE Brazil; Sr–Nd isotopes; Trindade plume track; South Atlantic*

INTRODUCTION

Most of the observational input to hypotheses about mantle plumes and their associated magmatism has come from studies of phenomena in ocean basins, where the lithospheric plates have both relatively uniform compositions and thicknesses that appear to conform well with those predicted by plate-tectonic theory. Even the thickest oceanic plates are thin enough to permit an underlying hot mantle plume to decompress sufficiently to produce 'dry' basaltic (*s.l.*) melt (e.g. Watson & McKenzie, 1991; Farnetani & Richards, 1995; Cordery *et al.*, 1997). Therefore a plate drifting over an essentially fixed-position mantle plume collects a linear belt of excess migrating magmatism (seamount chain or aseismic ridge) that defines a direction and velocity of absolute plate motion (Morgan, 1983). A nomenclature for terms referring to plume–plate interaction needs to be established at the outset, to prevent subsequent ambiguity. In this paper, lithospheric plates *drift* over fixed-position mantle plumes. The magmatism produced above the latter appears to an observer to *migrate* across the plate surface. Finally, a *plume-track* is a line on the surface of a plate that depicts that plate's movement, relative to a fixed plume below.

Belts of migrating magmatism are scarce in the continental geological record. This can hardly be because mantle plumes rarely impinge beneath continents. McKenzie (1984) pointed out that a rapidly rising mantle plume-head, originating at the core–mantle boundary, is essentially unaware whether it is upwelling beneath an ocean or a continent far above. Therefore, plumes should impact and impinge beneath continents as frequently, per unit area, as they are observed to occur within the ocean basins. Numerical models that suggest some long-timescale coupling between continental plates, especially very large ones, and plume spatial distribution (e.g. Richards *et al.*, 1997) do not invalidate this short-timescale relationship. The physical evidence for many sub-continental mantle plume impacts is found in large igneous provinces. It is the post-impact belts of migrating magmatism, formed as continents drift over the fixed stems or tails of mantle plumes (Davis, 1995), that are rare. Hill (1991), Thompson & Gibson (1991), Sleep (1996, 1997) and others have suggested that the relatively deep lithospheric roots of a craton might deflect the hot upwelling mantle of a plume to adjacent regions with thinner lithosphere. We shall argue below that this occurred in SE Brazil.

Continuing plume-related ocean-basin magmatism at Tristan da Cunha and Trindade–Martin Vaz has built islands above sea level that are linked by an aseismic ridge and a seamount chain, respectively, to the continental margin of SE Brazil. Plate reconstructions at ~135 Ma and ~85 Ma place the Tristan and Trindade 'hotspots', respectively, beneath or close to SE Brazil (Crough *et al.*, 1980; Hartnady & le Roex, 1985; Fleitout *et al.*, 1989; O'Connor & Duncan, 1990; Müller *et al.*, 1993), at times when magmatic activity also peaked (see below). Adopting the view that geologically younger magmatism in the adjacent South Atlantic ocean basin gives an *a priori* reason for suspecting mantle plume involvement in this Cretaceous magmatism, we have investigated whether straightforward application or extension of current theory can explain both the existing data and those accumulated by our own research (Thompson & Gibson, 1991, 1994; Gibson *et al.*, 1995, 1996, 1997*c*).

Gibson *et al.* (1995) showed that widespread strongly potassic alkaline magmatism in the Alto Paranaíba region (Fig. 1) was synchronous at ~85 Ma, the time that plate-tectonic reconstruction places the Trindade plume close to this region. They interpreted this as an example of a mantle plume that first impacted beneath continental lithosphere too thick to permit 'dry' decompression melting and hence basalt (*s.l.*) production. Instead, the volatile-rich alkaline magmas, including diamondiferous kimberlites, were generated by uplift and heating of the lithosphere above the plume head.

Gibson *et al.* (1997*c*) showed that the ~85 Ma magmatism extends as far NW as Mato Grosso (Fig. 1), where kimberlites (some diamondiferous) occur in cratonic areas but a pre-existing rift, i.e. a site of earlier lithospheric thinning, preserves alkali–olivine basalts of the same age. This is the way that the magmatism might be expected to behave when a starting-plume head, impacting beneath thick lithosphere, encounters a pre-existing local 'thins-pot' (Thompson & Gibson, 1991; Sleep, 1997).

In this paper we focus on alkaline magmatism in SE Brazil that post-dates the ~85 Ma Trindade starting-plume impact-related activity of Alto Paranaíba and Mato Grosso but pre-dates the oldest offshore volcanism at the landward end of the Trindade–Martin Vaz seamount chain. This younger activity built the Abrolhos Platform at 52–42 Ma (Cordani, 1970; Fodor *et al.*, 1989). We shall present evidence that, between ~85 and 55

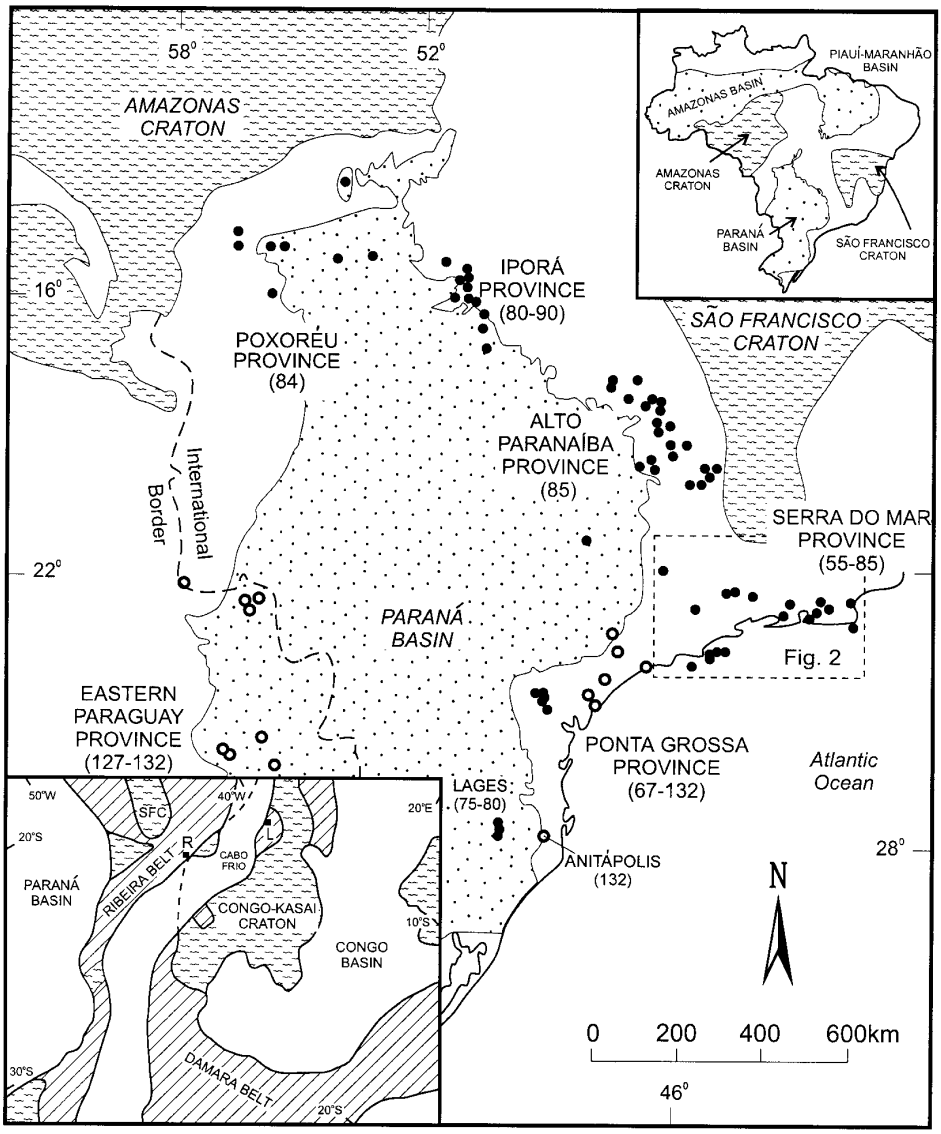

Fig. 1. Geological sketch map of SE Brazil showing the distribution of Cretaceous igneous centres and provinces around the margin of the Paraná sedimentary basin; modified from Ulbrich & Gomes (1981) and Schobbenhaus *et al.* (1984). Open and filled circles are Early and Late Cretaceous–Palaeogene complexes, respectively. Age ranges of magmatism (in parentheses) are derived from our published and unpublished determinations, together with published radiometric dates filtered for quality [see text and Gibson *et al.* (1995) for details and sources]. The top right inset shows the principal cratons and sedimentary basins of Brazil. The bottom left inset shows the principal structural units of SE Brazil and SW Africa in their pre-Jurassic Gondwana configuration [modified from Fonseca *et al.* (1995)]. SFC, São Francisco craton; R, Rio de Janeiro; L, Luanda.

Ma, the Trindade mantle plume tail passed beneath lithosphere of the Archaean São Francisco craton (Fig. 1) that was thick enough to prevent the generation of plume-derived magmas by decompression melting. Instead, we propose that part of the hot plume mantle was deflected several hundred kilometres southward, towards the thinned lithosphere of the continental margin, where it decompressed and generated an eastward migrating sequence of alkaline igneous complexes.

THE SERRA DO MAR IGNEOUS PROVINCE

Nomenclature

The Late Cretaceous to Early Tertiary complexes that are discussed in this paper occur along and near the SE Brazilian coast, between longitudes 42° and 47°W (Fig. 2). They form a distinct igneous province because further west, with the exception of the tiny (<1 km^2) ~85 Ma

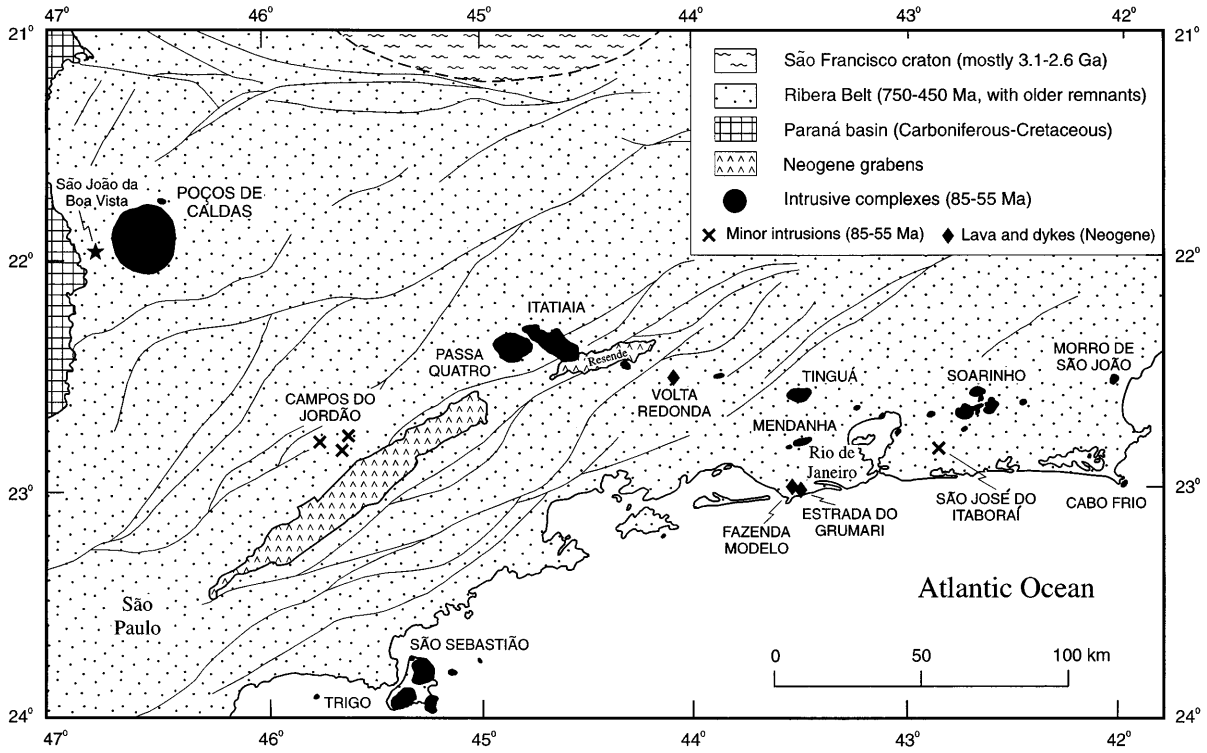

Fig. 2. Geological sketch map of the Serra do Mar igneous province; simplified from Schobbenhaus *et al.* (1984). The town of São João da Boa Vista marks one end of the traverses used in Figs 4 and 6.

syenite outcrop at Cananéia (24°58′S, 47°54′W), the alkaline complexes are mostly much older (~130 Ma). Previous Brazilian accounts (e.g. Ulbrich & Gomes, 1981) have tended not to treat this province as a single entity but instead to focus on individual complexes (e.g. Poços de Caldas) or small groups of complexes, such as São Sebastião and adjacent islands or the plutons around Rio de Janeiro. We hope that the following account will convince readers that that we are justified in grouping these complexes to form the Serra do Mar igneous province.

Geological setting

The metamorphic basement in the region of the Serra do Mar province comprises the partly Archaean São Francisco craton in the north and a mobile belt between this and the coast that gives radiometric dates as young as Lower Palaeozoic. The São Francisco craton has recently yielded ages amongst the oldest terrestrial rocks (Teixeira *et al.*, 1996), including a well-dated anorthositic sill at 3·12 Ga (zircon U/Pb) and evidence from both zircons and Rb/Sr systematics of gneisses that are as old as ~3·38 Ga. Before final stabilization, this craton underwent major reworking at 2·86–2·70 Ga and intrusion by granites between 2·7 and 2·6 Ga. Thereafter, its SE margin was again reworked between 2·4 and 2·0 Ga during the Transamazonian orogeny (Machado *et al.*, 1996). The youngest K–Ar mineral ages from this region are ~1·8 Ga (Teixeira *et al.*, 1996).

Between the São Francisco craton and the coast, the pattern of radiometric ages is entirely different. The results of Fonseca *et al.* (1995) and Machado *et al.* (1996) show that the majority of the published dates from this Ribeira belt fall in the range 750–450 Ma, spanning the Brasiliano–Pan-African orogeny. The remaining dates are older, up to 2·3 Ga, and suggest that some (possibly most) of this mobile belt is reworked Transamazonian basement. Many of these older dates come from the gneisses that outcrop around Cabo Frio and form the offshore island of Búzios (Fig. 2). Fonseca *et al.* (1995) suggested that these two localities are fragments of the reworked eastern margin of the Congo–Kasai craton, overprinted by the Brasiliano–Pan-African orogeny. Figure 1 (inset) illustrates this concept.

Teleseismic tomographic studies suggest that the lithospheric thickness beneath the São Francisco craton is 200–250 km (Grand, 1994; VanDecar *et al.*, 1995). The offshore basins along the Brazilian coast have all been

the subject of intensive geophysical studies, during hydrocarbon exploration programmes. The segment offshore from the Serra do Mar igneous province, the Santos basin, is a classic example of a continental passive margin, with strong crustal (and therefore presumably lithospheric) thinning related to rifting during the initial opening of the South Atlantic (e.g. Chang *et al.*, 1992; Mohriak *et al.*, 1995). Chang *et al.* (1992, table 1) gave an estimated average β factor of 2·88 for the Santos basin. Lithospheric thickness beneath the Ribeira belt has not been investigated geophysically. Nevertheless, geological studies show that it is reasonable to suppose that it is considerably thinner than the São Francisco craton. Thus Gresse *et al.* (1996) documented late- to post-orogenic basin formation throughout the Brasiliano–Pan-African belts of southern Africa and southern Brazil. Molyneux (1997) has shown that strong extension accompanied late Brasiliano granite emplacement in the Ribeira belt.

To the west of the Serra do Mar province the metamorphic basement is overlain by the deposits of the Paraná basin, which has had a multiphase extensional history since the Late Ordovician. The Poços de Caldas complex (Fig. 2) is the only unit of the Serra do Mar magmatism to intrude Paraná basin sediments locally, namely the Jurassic Botucatu sandstones. Finally, there are minor extensions of the Santos basin system onshore, as Middle Tertiary grabens within the Ribeira belt (Fig. 2). Their Neogene infillings include arenites, shales (some bituminous) and limestones (Klein & Valença, 1984; Schobbenhaus *et al.*, 1984).

Late Cretaceous igneous complexes

This study of Serra do Mar magmatism was aimed specifically at improving knowledge of its age and investigating the mantle sources of the alkaline magmas. Therefore both our fieldwork and the following account are selective. The bulk of the complexes is a range of syenites, sometimes accompanied by trachytes and/or phonolites. Associated mafic rocks are uncommon and mostly confined to dykes. Woolley (1987) gave an excellent overall account of these complexes, summarizing all previous publications. Subsequent contributions have come from Bellieni *et al.* (1990), Brotzu *et al.* (1992, 1995, 1997), Shea (1992), Regelous (1993), Amorim *et al.* (1995), Araújo *et al.* (1995), Garda *et al.* (1995), Montes-Lauar *et al.* (1995), Morbidelli *et al.* (1995) and Valente *et al.* (1995). We shall describe the syenites and other felsic rock-types in general terms and then give more detailed accounts of the mafic rock-types sampled during this study.

Syenites and related rock-types

The syenite–phonolite-dominated complexes range in size from small isolated phonolite plugs to Poços de Caldas (800 km^2), the largest alkaline complex in Brazil and one of the largest in the world. The smaller Itatiaia complex (330 km^2) is equally impressive, as it forms a 31 km × 12 km rugged mountain massif, 2787 m in height. Many of the other syenite complexes (e.g. Tinguá, Rio Bonito, Soarinho and Morro de São João, Fig. 2) also form spectacular forest-clad peaks. Small remnants of the volcanic superstructures of these plutonic complexes are preserved locally (Woolley, 1987): Poços de Caldas includes tuffs, breccias, agglomerates and mafic to phonolitic lavas; Tinguá includes phonolitic lavas and tuffs; Mendanha comprises predominantly volcanic agglomerates, tuffs and breccias, containing clasts of a wide range of alkaline rock-types, together with ignimbrites (Klein *et al.*, 1984). Thus, the Serra do Mar plutonic complexes most probably originated beneath a chain of alkaline volcanoes comparable with those along the East African rift system. The volcano capping Itatiaia may have resembled the present-day Mts Kenya and Kilimanjaro, and Poços de Caldas may have underlain a similar-sized or even larger volcano or volcano group; it is thought to be encircled by a caldera fault ~33 km in diameter (Schorscher & Shea, 1992).

The majority of the syenites (Woolley, 1987) contain abundant nepheline, although others are nepheline free. Some have biotite and green amphibole as their main ferromagnesian minerals, accompanied by melanite garnet in the Rio Bonito, Tinguá and Morro de São João complexes. Other common members of all the felsic complexes are peralkaline syenites–phonolites, with sodalite, aegirine, arfvedsonite and occasionally eudialite. Despite the impression given by their mineralogy and chemical compositions (e.g. Bellieni *et al.*, 1990; Brotzu *et al.*, 1992), the syenites may originally have been considerably more potassic than they appear to be at present because pseudoleucite is widespread (Woolley, 1987), with leucite-shaped polyphase pseudomorphs composed of orthoclase, nepheline and zeolites, together with minor amphibole, muscovite and carbonate (Valença & Edgar, 1979). These are especially abundant in the Morro de São João complex, where we have observed individual pseudomorphs up to 4 cm in size. The largest known pseudoleucites in this province are 29 cm at Tinguá (Lima, 1976). Post-crystallization alteration of leucite strongly affects the K/Na ratio of the rock (e.g. Thompson *et al.*, 1997*c*).

It has been generally considered that the Serra do Mar province syenites–phonolites originated by fractional crystallization from mafic parental magmas (Woolley, 1987). These melts are specified in recent published accounts to be silica undersaturated and relatively sodic basanite–tephrites (Bellieni *et al.*, 1990), basanite (Brotzu *et al.*, 1992, 1995) or camptonite and soda vogesite (Araújo *et al.*, 1995). Nevertheless, both Brotzu *et al.* (1992, 1995, 1997) and Amorim *et al.* (1995) noted that the syenites–

phonolites of the Serra do Mar province have significantly higher K_2O/Na_2O ratios than those within the older complexes of the Ponta Grossa province to the SW (Fig. 1), and they speculated that the Serra do Mar mafic parental magmas may likewise be relatively potassic. Schorscher & Shea (1992) made the same point and invoked a 'primary magmatic perpotassic characteristic' in the parent magma at Poços de Caldas.

Mafic rock-types

The mainland igneous complexes of the Serra do Mar province form an approximately linear array, ~500 km in length, from Poços de Caldas to Cabo Frio. Another group is exposed as offshore islands along the coast south of Poços de Caldas (Fig. 2). The following account summarizes our own observations. The mafic–ultramafic rock-types occur in four situations in this province: (1) dykes within the country rock up to ~10 km away from each complex, although most of these are felsic; (2) dykes cutting the syenites and associated felsic central plutons; (3) lavas and agglomerate blocks within remnants of volcanic superstructures; (4) layered gabbros associated with the syenites (in two instances). Coastal SE Brazil is a subtropical region with high rainfall. Consequently, lateritization is frequently intense and affects all rock-types on low ground. Mafic samples suitable for igneous geochemistry are confined to river gorges, coastlines, quarries and some roadsides.

Poços de Caldas. Brecciated lavas, polylithic agglomerates and tuffs are exposed for ~14 km along the road between Cascata and Águas da Prata. The mafic blocks are feldspar-free leucitites, containing phenocrysts of clinopyroxene, leucite (also in the groundmass) and magnetite (see Table 2, 90SB68), olivine (90SB66, 67, 72, 79) and occasional phlogopite (90SB64); all phases are variably altered. The Osamu Utsumi open-cast uranium mine intersects several fresh mafic potassic dykes, cutting hydrothermally altered phonolites. Shea (1992) and Waber *et al.* (1992) discussed the petrography, geochemistry and classification of this rock-type but did not give chemical analyses. Judging from the description given, their proposal that these dykes are lamproites is perhaps incorrect, in the light of current nomenclature (Woolley *et al.*, 1996). They are probably kamafugites, an extremely common rock-type in the penecontemporaneous Alto Pananaíba igneous province (Gibson *et al.*, 1995), immediately to the north (Fig. 1).

Campos do Jordão. The Campos do Jordão region lacks a well-defined intrusive complex and major occurrences of leucocratic rock-types. Instead it includes the Ponte Nova pluton, a sill or stock of alkaline gabbro to picrite, and a scattered swarm of basalt (*s.l.*) to picrite dykes, up to 1 m in width. The Ponte Nova pluton is predominantly nepheline melagabbro, with associated leucogabbros and syenitic veins. It is cut by dykes ranging from micromelagabbro to phonolite (93SOB205, 206), and also by members of the swarm (93SOB198). All the dykes in the swarm are feldspar-free olivine melanephelinites. They have olivine and clinopyroxene phenocrysts (93SOB198, 208–13), sometimes accompanied by megacrysts of clinopyroxene (198, 213), olivine and phlogopite (213). Groundmass minerals are clinopyroxene, olivine, opaques and minor amphibole and biotite, in a matrix of nepheline (in the two picrites, 208, 209) or glass (in the other samples).

Passa Quatro. A quarry in metamorphic basement gneiss adjacent to this complex is cut by two mafic alkaline dykes trending 280° (94SOB90–92), containing clinopyroxene, olivine and magnetite phenocrysts (plus amphibole and phlogopite in 90), together with apatite microphenocrysts, in a groundmass of clinopyroxene, amphibole, biotite, opaques and local alkali feldspar, with interstitial glass.

Itatiaia. Mafic dykes were found cutting the syenites at two localities. Between Moringa and Cachoeira a 2 m wide dyke (94SOB95) contains spinel lherzolite xenoliths, olivine and clinopyroxene phenocrysts in a groundmass of these phases, opaques, plagioclase and interstitial glass. At the eastern end of the complex the road from Resende ascends the scarp of the Resende graben (Fig. 2) and exposes several mica-rich dykes (94SOB97, 98). These have clinopyroxene and magnetite phenocrysts (97) or clinopyroxene, olivine and phlogopite microphenocrysts (98), in a groundmass of these phases, amphibole, alkali feldspar, apatite and glass.

Tinguá. The upper slopes of Tinguá are densely forested and there is thick laterite around the base. Fresh leucocratic dykes are abundant but only one mafic example was found; a weathered 2 m wide minette (*s.l.*) with fresh phlogopite and altered olivine and clinopyroxene phenocrysts, exposed during 1994 land clearance at 22°37′19″S, 43°26′21″W.

Mendanha. Dykes from the swarms surrounding this complex are excellently exposed in large quarries within the metamorphic basement gneisses at Sentíssimo, Bangu and Nova Iguaçu. Most of the dykes trend 245°–260° but a sub-set at Nova Iguaçu trends 225° and one cross-cutting dyke at Sentíssimo trends 140°. Valente *et al.* (1995) recorded mafic alkali–olivine basalts, basanites, tephrites, nephelinites, trachytes and phonolites in the Rio de Janeiro area. Of the dykes collected during the present study, the Nova Iguaçu suite includes intermediate and trachytic members, but most are mafic–ultramafic. Plagioclase-rich basaltic dykes occur sparsely in the swarm but all analysed samples (see Table 2) are plagioclase poor to plagioclase free, with phenocrysts of olivine and clinopyroxene, joined by chromite in the picrites (94SOB64, 66, 67). Olivine phenocrysts are less abundant in more evolved compositions (68, 78, 80) and phenocrysts of magnetite, phlogopite, amphibole (57, 58,

61) and apatite (81) join the clinopyroxene. The two sodic Bangu picrites (66, 67) have clinopyroxene phenocrysts with green cores and groundmass clinopyroxene, olivine, opaques and amphibole, together with only traces of biotite. The other samples have the same groundmass phases (plus interstitial glass) but in 58 and 81 there is plentiful biotite and no amphibole.

São José do Itaboraí. Klein & Valença (1984) described 'ankaramitic' dykes and pillow lavas within the Late Cretaceous to Palaeocene limestones filling a small graben. Exposure is minimal. The two samples analysed in this study both have olivine, titanaugite and chromite phenocrysts (94SOB50, 51). Some of the clinopyroxene phenocrysts in 51 have bright green centres. The groundmass in both samples contains olivine, clinopyroxene and opaques, together with accessory plagioclase, apatite and interstitial zeolite; biotite is also prominent in 50.

Tanguá, Rio Bonito and Soarinho. Although trachyte and phonolite dykes are abundant around this cluster of complexes, fresh mafic samples were only found NW of Soarinho, as boulders eroded from dykes cutting metamorphic basement in a river gorge. They are all minettes, with phenocrysts of phlogopite either alone (94SOB131) or plus olivine (127), together with magnetite, apatite and sanidine (128, 129). Their groundmasses are all rich in biotite and sanidine.

Morro de São João. Published accounts (Woolley, 1987) mention ultramafic rock-types at this centre but the most mafic sample located in this study is a nepheline melasyenite (94SOB142).

Cabo Frio. Abundant trachyte and phonolite dykes, with sanidine, phlogopite, nepheline and leucite phenocrysts, are exposed on the sea cliffs around this complex. We located three thin (<1 m) dykes that are considerably more mafic than those reported previously (Araújo *et al.*, 1995). Two have clinopyroxene and olivine phenocrysts, with groundmass of clinopyroxene, opaques, plagioclase, nepheline(?), amphibole and apatite (93SOB193, 197). One has additional phlogopite phenocrysts and a groundmass of clinopyroxene, opaques, biotite, apatite and devitrified glass (196).

Trigo. This offshore island is composed of both nepheline syenite and cumulus-textured, layered alkali gabbro. Mafic to leucocratic dykes are relatively common along its coast. The mafic dykes have olivine and clinopyroxene phenocrysts (94SOB14, 17, 20), with groundmass plagioclase (plus nepheline in 14), amphibole, biotite and opaques, plus accessory apatite. Amphibole, magnetite and apatite join the phenocryst assemblages in more evolved compositions.

São Sebastião (Ilhabela). The island of São Sebastião, also known as Ilhabela, lies offshore from the mainland port of São Sebastião and a stretch of coast rich in alkaline mafic dykes. The latter have been studied in detail by Regelous (1993) and Garda *et al.* (1995). The metamorphic basement of Ilhabela is cut by three syenite stocks and a small cumulus-textured layered gabbro that contains hypersthene. Alkaline dykes occur in the basement areas and also cut the syenites. On the NE coast it is clear that post-syenite mafic dykes were emplaced before the syenite was completely solidified; the dykes have broken into joint blocks that have subsequently rotated. In basement areas, the alkaline dykes have to be separated from large numbers of tholeiitic quartz dolerites belonging to a coast-parallel Paraná swarm, 129–136 Ma in age (Regelous, 1993), that is prominent throughout the coastal region of Fig. 2. Fortunately, the tholeiites are distinctive petrographically and on Ilhabela they are clearly metamorphosed by the syenites. The Ilhabela alkaline dykes analysed for this study have titanaugite and olivine phenocrysts (90SB54, 94SOB31), in a groundmass of clinopyroxene, olivine, opaques, apatite and interstitial zeolite and carbonate (90SB54), or amphibole, biotite, plagioclase, clinopyroxene, opaques and apatite (94SOB31). The groundmass texture of the latter sample is equigranular and hornfelsic (beerbachitic), consistent with the field evidence (above) that some of these dykes penetrated still-hot syenite. The mainland São Sebastião coastal mafic dykes mostly trend ~150° and are aphyric (94SOB12), or have olivine phenocrysts (13), or clinopyroxene microphenocrysts (10). The groundmass of the picrite (13) is exceedingly fine grained but seems to have the same essential phases as the other dykes: clinopyroxene, olivine, biotite, opaques, apatite, sodic plagioclase (12) and pseudomorphs after a mineral with the shape of nepheline (10). Garda *et al.* (1995) recorded melilite in one coastal dyke.

Mafic alkaline magmatism of Mid-Tertiary and uncertain age

At first sight this topic falls outside the scope of the paper. But the mid-Tertiary basalts (*s.l.*) of coastal SE Brazil (Fig. 2) potentially throw light on the geochemistry of the preceding Serra do Mar magmatism because some of them contain spinel lherzolite xenoliths. They may therefore offer a chance to deduce the nature of the mantle beneath this region, once it had drifted well clear of the Trindade mantle plume.

Volta Redonda. A small graben, 4·5 km SE of Volta Redonda, strikes ~290° and is infilled with Neogene Resende Formation sediments, including a basaltic lava flow and associated agglomerates. The lava (94SOB89) has phenocrysts of olivine, titanaugite and chromite, in a groundmass of olivine, clinopyroxene, opaques, accessory apatite, and interstitial plagioclase and zeolite.

Estrada do Grumari and Fazenda Modelo. Fragments of two lherzolite xenolith bearing basaltic dykes along the coast west of Rio de Janeiro (Fig. 2) are of unknown age but

closely resemble the Volta Redonda lava. Both have olivine, titanaugite and chromite phenocrysts (94SOB55, 56), together with lherzolite xenoliths (plus feldspar xenocrysts in 55). Their groundmasses are composed of clinopyroxene, olivine, opaques, plagioclase and apatite.

Resende. This relatively large graben (Fig. 2) has no associated igneous rocks but, as the Itatiaia complex borders it to the north, it is conceivable that the Itatiaia dyke (94SOB95), which closely resembles 94SOB55, 56 and 89, may also have a Mid-Tertiary age. Currently its age is unproven.

RADIOMETRIC AGES OF SERRA DO MAR PROVINCE MAGMATISM

In this section we summarize published radiometric dates, critically assess them and discuss them in the light of new determinations.

Published dates

The Mesozoic and Early Tertiary alkaline magmatism of southern Brazil and Paraguay has been the subject of many radiometric dating programmes during the last three decades. Compilations of these dates, with or without discussions of their significance, include those of Herz (1977), Ulbrich & Gomes (1981), Woolley (1987) and Sonoki & Garda (1988). The Sonoki & Garda paper was a benchmark because it listed all previous K/Ar dates, at a time when few determinations by other techniques were available. The number of new radiometric dates published since has been small but these include a higher proportion by such techniques as Rb/Sr isochrons and $^{40}Ar/^{39}Ar$ (see below).

A histogram of all the Sonoki & Garda (1988) dates (Fig. 3) shows two clear peaks, at 130–140 Ma and at 80–90 Ma. Recent papers have used $^{40}Ar/^{39}Ar$ and Rb/Sr techniques to show that 130–140 Ma corresponds to the Paraná–Etendeka flood-basalt event (e.g. Regelous, 1993; Milner *et al.*, 1995; Renne *et al.*, 1996; Turner *et al.*, 1996). There is widespread, although not unanimous (e.g. King & Anderson, 1995), agreement that this flood-basalt province was generated directly or indirectly in response to the initial impact of the mantle plume now sited beneath Tristan da Cunha. In contrast, there has been considerable reluctance to consider a similar model for the late Cretaceous and younger alkaline magmatism. Gibson *et al.* (1994, 1995, 1997*c*) have shown that a combination of new radiometric dates and careful checking of the quality of published ones indicates that the alkaline magmatism (kamafugites, kimberlites, lamproites and local basalts) throughout the large area of Alto Paranaíba, the Iporá–Rio Verde region of southern Goiás, and the adjacent part of Mato Grosso (Fig. 1) all occurred in the 80–90 Ma timespan, with a peak at ~85 Ma. They attributed this widespread synchronous magmatism to the initial impact of the mantle plume that is currently beneath Trindade–Martin Vaz.

If the <100 Ma dates in the Sonoki & Garda (1988) compilation from the Alto Paranaíba, Iporá and Mato Grosso regions are excluded, the majority of the remainder are samples from the Serra do Mar province. This alkaline magmatism has generally been attributed to passive continental margin extension (e.g. Ulbrich & Gomes, 1981; Brotzu *et al.*, 1995; Morbidelli *et al.*, 1995). One of our main initial objectives was to investigate whether the Serra do Mar province magmatism occurred synchronously or in a random time pattern, as might be expected if it resulted from plate-margin extension, or whether it initiated progressively later from west to east, as would be consistent with the South American plate drifting over a mantle plume. Use of the data in the Sonoki & Garda (1988) compilation unscreened and alone appears marginally to support the extension model. Figure 4 shows the age ranges for each Serra do Mar province complex, projected onto a line between São João da Boa Vista and Cabo Frio (Fig. 2). It should be noted that, although most of the centres fall relatively close to this line, the offshore islands of Trigo, São Sebastião (Ilhabela), Vitória and Búzios lie far to the south. The unscreened data shown in Fig. 4 imply that several of the Serra do Mar volcanoes were active for about an order of magnitude longer than either any known Pliocene–Recent volcanoes or volcano groups, or older volcanic centres that have been dated accurately by the best current techniques (e.g. Milner *et al.*, 1995; Renne *et al.*, 1996; Pearson *et al.*, 1998). It is therefore appropriate to assess the Sonoki & Garda (1988) compilation rigorously.

Our first step has been to reject all the bulk-rock K/Ar dates in the compilation. Obviously this will result in the loss of some good data but experience of the bulk-rock K/Ar dating of very similar rock-types in the Alto Paranaíba province (Gibson *et al.*, 1994, 1995, and unpublished data, 1996) has convinced us that this technique is not reliable for SE Brazilian Cretaceous–Tertiary alkaline igneous rocks. The widespread leucite in the mafic, strongly potassic types is mostly variably altered to analcite and other phases (e.g. Cima, 1995). Our study of the Serra do Bueno dyke in the Alto Paranaíba province (Fig. 1), which contains altered groundmass leucite, showed graphically the effect of this alteration on K/Ar dating (Gibson *et al.*, 1994). Our own and published bulk-rock dates (Woolley, 1987) are similar (37 and 45 Ma, respectively) but far less than the laser $^{40}Ar/^{39}Ar$ age of 90 Ma; the latter is consistent with other high-reliability dates throughout this province (Gibson *et al.*, 1995). Altered leucite is common in the syenites of

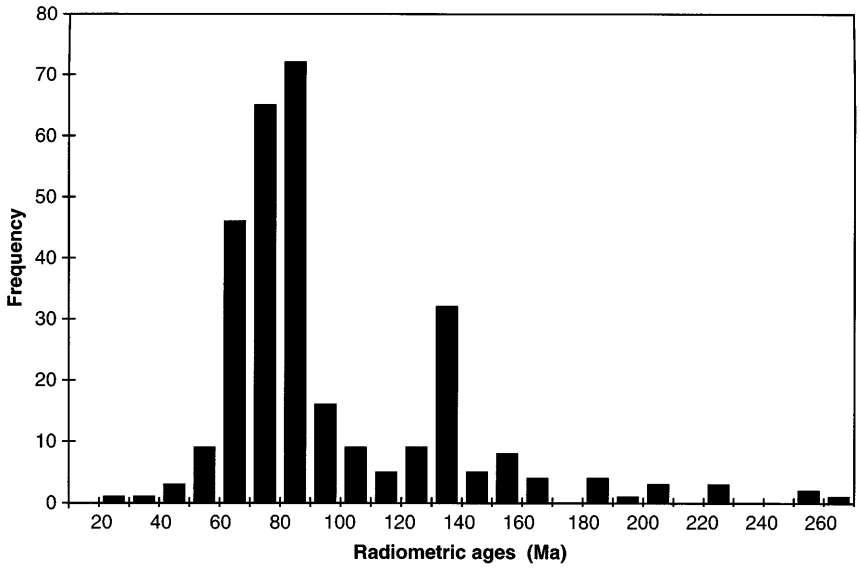

Fig. 3. Histogram of all published pre-1988 radiometric dates of Mesozoic and Tertiary alkaline rocks in SE Brazil; compiled by Sonoki & Garda (1988).

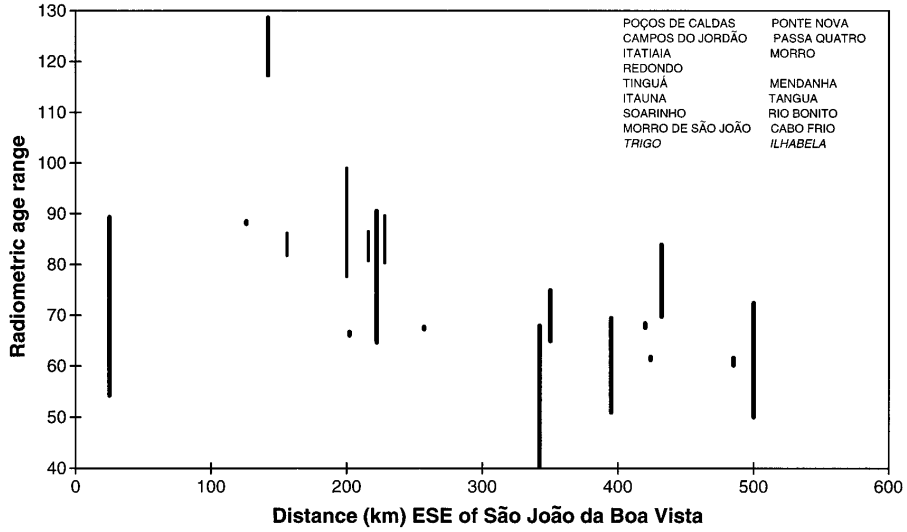

Fig. 4. Ranges of all published pre-1988 radiometric dates (Sonoki & Garda, 1988) for Serra do Mar province igneous complexes. All data are projected onto a line between São João da Boa Vista and Cabo Frio (Fig. 2). Age ranges of complexes close to the line (see list on diagram) are plotted as thick vertical bars. Age ranges of the four coastal or offshore complexes around São Sebastião, far south of the line (Fig. 2) are plotted as thinner bars and listed in italic.

the Serra do Mar central complexes (see above) and petrographic evidence abounds for their pervasive post-crystallization hydrothermal alteration. This process continues to the present day; the Araxá (Alto Paranaíba) and Poços de Caldas complexes are both sites of hot-spring-fed spa resorts. Shea (1992) specified that hydrothermal alteration at Poços de Caldas has reset radiometric ages within the complex. Therefore we have also rejected all feldspar K/Ar dates from central-complex plutons within the Sonoki & Garda (1988) compilation. Again, this procedure will exclude some reliable dates but it is very difficult to see how else to screen the published ages.

The remaining Sonoki & Garda dates were obtained using separated biotite, amphibole and pyroxene. The few published amphibole K/Ar dates seem to be consistent with the most reliable biotite ages (see below) and the results by other techniques, such as $^{40}Ar/^{39}Ar$.

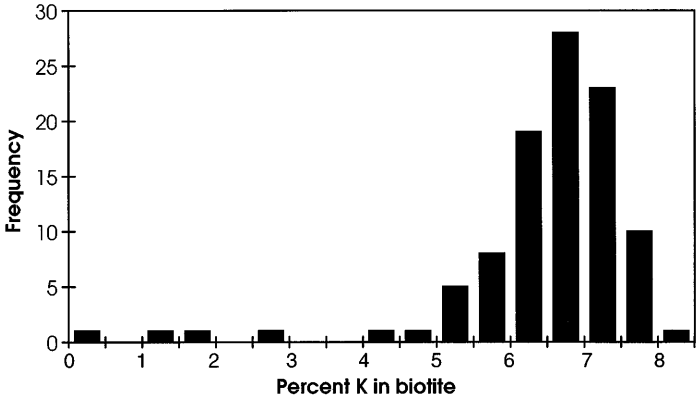

Fig. 5. Potassium contents (% K) of biotites used in all the published pre-1988 biotite K/Ar dates compiled by Sonoki & Garda (1988).

This is not so for the pyroxene K/Ar dates, which give variable (mostly high) ages for complexes such as Jacupiranga, São Paulo State, where $^{40}Ar/^{39}Ar$ ages are available (Renne *et al.*, 1993). Many biotite dates are listed in the Sonoki & Garda (1988) compilation and it is also well established that this mineral is comparatively resistant to low-temperature hydrothermal alteration. We have therefore screened the Sonoki & Garda compilation, by comparing the potassium contents of the dated micas with the known K_2O ranges of fresh syenite biotites (8–9 wt %; Deer *et al.*, 1965) and the phlogopites–biotites of mafic potassic rock-types (9–11 wt %; Mitchell & Bergman, 1991), using the compositions of 'separable' crystals rather than groundmass or rim analyses. Sonoki & Garda (1988) gave biotite potassium contents in weight percent K and Fig. 5 is a histogram of these values; 8% K_2O equates with 6·6% K in Fig. 5 and it is therefore clear that many of the published phlogopite–biotite K/Ar dates listed by Sonoki & Garda used material that was either severely altered to chlorite or a poor mineral separate, or both. Consequently, we have recompiled these dates, after eliminating all 'micas' that fail a crude test of realistic K content. In an effort to try to avoid 'borderline', less-than-ideal samples, we have rejected all Sonoki & Garda phlogopites–biotites with <7% K (8·4% K_2O). This is an extremely severe criterion for locating only fresh phlogopites–biotites and it has undoubtedly resulted in our rejection of several perfectly good published dates. The purpose of our ultra-severe screen is to convince readers that the remaining published K/Ar dates which we use are reliable.

Figure 6 shows the remaining (accepted) phlogopite–biotite dates plotted along the same traverse as Fig. 4, together with results from Rb/Sr isochrons that used carefully chosen bulk-rock samples (e.g. Brotzu *et al.*, 1989, 1992; Shea, 1992), $^{40}Ar/^{39}Ar$ dates (Shea, 1992; Regelous, 1993) and new K/Ar results of our own. These will be described before returning to Fig. 6.

New phlogopite–biotite phenocryst K/Ar dates

In our studies of Brazil–Paraguay alkaline igneous rocks (e.g. Gibson *et al.*, 1995) we have discovered one method to obtain some excellent K/Ar dates in provinces, such as Serra do Mar, where altered leucite is widespread and the magmatism is dominated by intrusive complexes that are affected by powerful long-lived hydrothermal activity. Occasional lavas and hypabyssal plutons contain fresh phlogopite–biotite phenocrysts which are extracted *in the field*. Individually checked phenocryst fragments are then crushed for K/Ar analysis.

Regelous (1993) used this approach in the Serra do Mar province, to obtain a date of 80·1 Ma by $^{40}Ar/^{39}Ar$ for the phenocryst biotite in a Campos do Jordão dyke (Fig. 2). We have located two felsic dykes (Mendanha and Cabo Frio) and one minette (Cabo Frio) that yielded suitable micas for K/Ar dating of field-separated phenocryst fragments, plus two minettes (Soarinho) with abundant, easily separated biotite. The results are listed in Table 1 and plotted in Fig. 6. One of the Soarinho biotite separates in Table 1 (94SOB131) actually fails the K_2O criterion used for filtering published dates in the previous section, but is included because it gives a date concordant with that of another better sample (94SOB128) from the same locality. When combined with the filtered previous dates, the new results show a clear pattern of migrating age of magmatism, ESE across the Serra do Mar province (Fig. 6). Although the 'offshore islands' (Trigo, São Sebastião–Ilhabela, Vitória and Búzios) fit this trend reasonably well, it should be remembered that

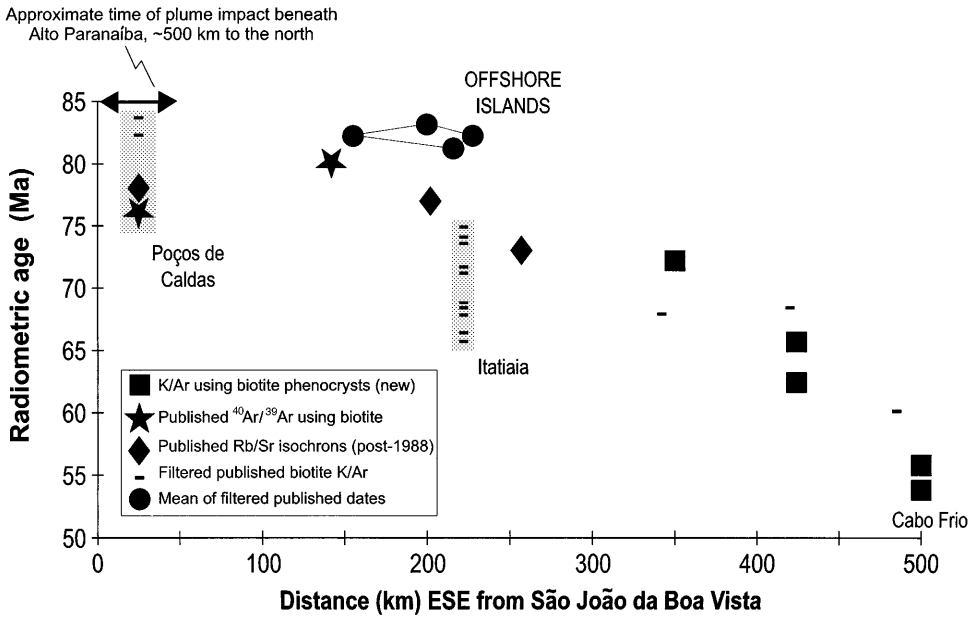

Fig. 6. New (Table 1) and published, high-quality, post-1988 radiometric dates for Serra do Mar province igneous complexes. Filtered older published biotite K/Ar dates are also plotted (see text for details of the screening procedure). Poços de Caldas and Itatiaia–Passa Quatro are by far the largest Serra do Mar province complexes (Fig. 2). The 'Offshore Islands' complexes, Trigo, São Sebastião, Búzios and Vitória, lie considerably to the south of the line between São João da Boa Vista and Cabo Frio (Fig. 2), onto which the data are projected. Sources of published dates are Sonoki & Garda (1988), Brotzu *et al.* (1989, 1992), Shea (1992) and Regelous (1993).

Table 1: Potassium–argon ages of phlogopites

Locality	Sample no.	K_2O (wt %)	Radiogenic ^{40}Ar (mm^3/g)	Atmospheric contamination (%)	Age (Ma ± 1σ)
Nova Iguaçu	94SOB72a	8·66 ± 0·04	(2·03 ± 0·05) × 10^{-2}	30·7	71·2 ± 1·8
(Mendanha)*	94SOB72b		(2·09 ± 0·04) × 10^{-2}	20·5	73·3 ± 1·4
Soarinho†	94SOB128	8·79 ± 0·10	(1·80 ± 0·02) × 10^{-2}	42·3	62·4 ± 1·0
	94SOB131a	7·87 ± 0·10	(1·70 ± 0·02) × 10^{-2}	44·5	65·7 ± 1·1
	94SOB131b	7·63 ± 0·09	(1·63 ± 0·02) × 10^{-2}	47·7	64·8 ± 1·1
Cabo Frio*	93SOB191a	8·91 ± 0·21	(1·62 ± 0·011) × 10^{-2}	25·4	55·5 ± 1·4
	93SOB191b		(1·64 ± 0·011) × 10^{-2}	38·8	56·2 ± 1·4
	93SOB196a	9·31 ± 0·16	(1·64 ± 0·011) × 10^{-2}	33·8	53·8 ± 1·0
	93SOB196b		(1·64 ± 0·011) × 10^{-2}	31·2	53·8 ± 1·0

*Hand-picked phenocrysts.
†Separates.
Details of analytical procedures have been given by Wilkinson *et al.* (1986). K_2O is the mean of five analyses. Decay constants are from Steiger & Jäger (1977).

they lie far to the south of other complexes at the same longitude (Fig. 2). The relatively long timespans of the magmatism at Poços de Caldas (~8 Ma) and Itatiaia (~10 Ma) may be related to the much larger sizes of these two complexes than the others. Gallagher *et al.* (1994) have reported apatite fission-track dates from metamorphic basement samples adjacent to Poços de Caldas that are consistent with the view that magmatism began at ~80 Ma and had cooled to <60°C after a few million years. Where high-quality data are available, large former volcanic complexes show magmatic activity age spans of no more than ~5–6 my. Examples are the Cretaceous Damaraland complexes, Namibia (Milner *et al.*, 1995; Renne *et al.*,

1996), and the Palaeocene Skye centre, Scotland (Pearson *et al.*, 1998). Nevertheless, the initiation of alkaline magmatism across the Serra do Mar province seems to lie on a well-defined trend.

GEOCHEMISTRY OF THE MAFIC ROCKS

Elements

The samples were analysed by a combination of X-ray fluorescence (XRF), instrumental neutron activation analysis (INAA) and inductively coupled plasma mass spectrometry (ICP-MS). Full details of our techniques used for XRF, INAA, and Sr- and Nd-isotopic ratios, were published by Gibson *et al.* (1995). Details of our ICP-MS techniques are given in Appendix B. Despite intense sub-tropical weathering in parts of the region, it is apparent that many of the analysed samples (Table 2) have loss-on-ignition (LOI) values of <5 wt %. The main exceptions are: (1) mica-rich rocks; (2) agglomerate blocks from Poços de Caldas, with leucite altered to analcite; (3) the thin dykes at Campos do Jordão. Amphibole also contributes to LOI in many samples. Obviously the geochemistry of the high-LOI, mica-poor samples needs to be treated with caution but otherwise these rocks are remarkably fresh in thin section, apart from altered olivine.

Figure 7 is a plot of $Na_2O + K_2O$ vs SiO_2 (TAS). Most of the samples in Table 2 classify as basanites (Le Maitre, 1989), consistent with their mineralogy. The petrographic identification of some of the Campos do Jordão dykes as melanephelinites is also borne out by their TAS compositions. Analyses of Trindade lavas in Fig. 7 (Halliday *et al.*, 1992; J. C. Greenwood, unpublished data, 1997) fall in the same TAS range as the Serra do Mar data. All the Poços de Caldas lavas contain leucite variably altered to analcite and this may have affected their compositions. Serra do Mar samples that contain phlogopite–biotite phenocrysts are noted in Fig. 7 and show high total alkali contents, relative to other samples with similar SiO_2.

$K_2O/(Na_2O + K_2O)$ ratios of most of the Serra do Mar samples (Fig. 8) fall in the same range as the available Trindade data but, at a given SiO_2 value, a small number of analyses are notably more potassic. All are mica-phyric except a Poços de Caldas leucitite (90SB79), the Morro de São João leucite-bearing melasyenite (94SOB142), and a São Sebastião picrite dyke (94SOB13). This picrite shows no petrographic evidence of its potassic composition and we shall discuss it further below, in the light of isotopic data. Turning to the relatively sodic compositions, the Mendanha and Neogene basalts–basanites with ~45% SiO_2 need no comment but the 'sodic' Poços de Caldas 'leucitites' show vividly the effects of analcitization on K/Na ratios.

Other aspects of the major-element compositions of the Serra do Mar samples are illustrated by Fig. 9, a plot of TiO_2 and CaO vs MgO. Although there are no signs of a single, overall Serra do Mar geochemical trend, most of these data behave in a coherent way, when the sub-sets from individual localities are considered. It should be noted that the apparent preponderance of relatively MgO-rich samples is an artefact of searching carefully for them in a syenite-dominated province. TiO_2 vs MgO in the Trindade and Campos do Jordão data sets (Fig. 9a) show similar inverted-V trends; the inflections at ~7% MgO correspond to the appearance of titanomagnetite microphenocrysts. Other Serra do Mar suites (Fig. 9b) form a scatter at MgO <9% and a single linear array at higher MgO abundances. The latter is a plausible olivine control line. CaO vs MgO (Fig. 9c) shows all data fitting a single scattered inverted-V trend, with its inflection at ~9% MgO. We interpret Fig. 9 as evidence that the compositions of the Serra do Mar mafic magmas are controlled by fractional crystallization: olivine (plus minor chromite) at >9% MgO; joined by Ca-rich clinopyroxene at <9% MgO and titanomagnetite at <7% MgO. The difference in TiO_2 abundance, at a given MgO value, between Trindade, Itatiaia, Poços de Caldas and Campos do Jordão samples, on the one hand, and São Sebastião–Trigo, Mendanha, Cabo Frio and Neogene samples, on the other, could be caused by either different mantle sources or different conditions during melting of a uniform source (see below).

Samples with MgO >6% are plotted in Fig. 10, La/Ba vs La/Nb, together with the field that encloses a large set of ocean-island basalts (OIB; Fitton *et al.*, 1991). Fitton *et al.* showed that this plot discriminated well amongst western USA Cenozoic basic volcanic rocks; those that were OIB-like, in terms of other elemental and isotopic criteria, fell within the OIB field whereas those that fell outside had other geochemical features suggesting a lithospheric contribution to their compositions. Clearly this plot cannot discriminate Cretaceous mafic magma sources so successfully in SE Brazil because the Alto Paranaíba kamafugites, which are inferred to be predominantly or entirely from lithospheric mantle sources (Gibson *et al.*, 1995; Carlson *et al.*, 1996), overlap the OIB field. Only one potassic Serra do Mar sample, Soarinho minette 94SOB131, plots far outside the OIB field.

Normalized incompatible-element plots (Fig. 11) allow comparison of a wide range of elemental abundances and ratios in mafic Serra do Mar samples and representative OIBs. The three mantle xenolith-bearing Neogene samples are clearly extremely similar geochemically and also OIB-like, resembling a basanite from Tenerife (Thompson *et al.*, 1984) and olivine melanephelinite from

Table 2: Representative whole-rock analyses

	Main WNW–ESE trend of Serra do Mar igneous centres												
Locality:	Poços de Caldas	Poços de Caldas	Poços de Caldas	Poços de Caldas	Poços de Caldas	Poços de Caldas	Poços de Caldas	Campos do Jordão (Ponte Nova)	Campos do Jordão (Ponte Nova)	Campos do Jordão (Ponte Nova)	Campos do Jordão	Campos do Jordão	Campos do Jordão
Occurrence:	Agglom-erate block	Agglom-erate block	Agglom-erate block	Agglom-erate block	Agglom-erate block	Agglom-erate block	Agglom-erate block	Dyke	Dyke	Dyke	Dyke	Dyke	Dyke
Sample no.:	90SB64	90SB67	90SB68	90SB70	90SB72	90SB75	90SB79	93SOB198	93SOB205	93SOB206	93SOB208	93SOB209	93SOB210
SiO_2	42·14	43·32	44·48	52·31	40·81	53·84	38·63	41·10	43·77	49·52	40·17	40·41	39·29
TiO_2	4·43	4·28	4·28	2·37	4·06	0·65	4·50	4·21	3·64	2·79	3·37	2·90	3·55
Al_2O_3	12·82	12·82	13·29	15·43	12·86	19·49	12·41	14·03	13·07	15·47	9·83	11·49	12·55
Fe_2O_3*	14·77	13·82	13·10	8·26	13·29	4·80	13·09	14·11	14·27	10·68	14·02	12·65	14·18
MnO	0·21	0·19	0·18	0·13	0·26	0·24	0·24	0·19	0·19	0·16	0·21	0·20	0·22
MgO	7·36	6·55	5·86	2·66	7·25	0·31	5·30	7·07	6·54	4·68	13·76	13·62	9·95
CaO	12·07	11·95	10·87	7·64	12·62	2·00	14·47	11·49	11·36	7·55	12·59	13·03	12·91
Na_2O	4·33	4·17	5·17	6·86	5·00	8·00	2·15	2·50	3·06	3·89	3·19	3·27	3·23
K_2O	0·63	1·28	1·43	2·52	1·91	8·38	6·05	2·94	2·19	3·31	1·78	1·41	1·76
P_2O_5	0·93	0·85	0·97	0·62	0·98	0·08	1·34	1·12	0·79	0·76	1·10	1·08	1·70
Total	99·68	99·24	99·64	98·79	99·04	97·79	98·18	99·03	99·06	99·02	100·02	100·06	99·33
LOI	5·68	2·71	4·11	6·85	13·02	0·77	8·87	5·02	0·63	5·13	6·83	5·25	7·77
Ba	653	1213	844	739	562	435	2136	1412	930	1159	1124	1353	1011
Cr	144	106	21	13	20	−2	50	158	54	72	369	370	127
Cs	3·36	—	2·70	—	—	—	1·70	0·80	0·80	0·87	—	2·60	4·10
Cu	64	75	51	20	64	5	102	48	101	34	41	51	33
Ga	26	19	21	16	14	37	25	22	23	27	16	18	21
Hf	8·99	8·54	10·43	9·19	10·09	—	9·14	7·18	6·53	8·43	8·69	6·84	10·06
Nb	110	99	138	94	131	252	180	104	74	75	110	118	126
Ni	93	61	48	22	35	3	26	75	97	52	364	257	113
Pb	7·17	8·00	7·13	—	—	—	4·53	5·44	4·96	9·42	—	4·95	6·02
Rb	40	23	42	29	41	165	142	73	49	84	39	71	71
Sc	23	29	20	11	14	0	21	26	26	16	25	29	25
Sr	807	1970	1059	1100	1251	1961	1536	1364	1009	1023	1119	1268	1767
Ta	6·53	5·54	8·46	5·26	—	—	9·01	5·98	4·25	4·20	7·10	6·86	8·21

Table 2: continued

	Main WNW–ESE trend of Serra do Mar igneous centres												
Locality:	Poços de Caldas	Poços de Caldas	Poços de Caldas	Poços de Caldas	Poços de Caldas	Poços de Caldas	Poços de Caldas	Campos do Jordão (Ponte Nova)	Campos do Jordão (Ponte Nova)	Campos do Jordão (Ponte Nova)	Campos do Jordão	Campos do Jordão	Campos do Jordão
Occurrence:	Agglomerate block	Agglomerate block	Agglomerate block	Agglomerate block	Agglomerate block	Agglomerate block	Agglomerate block	Dyke	Dyke	Dyke	Dyke	Dyke	Dyke
Sample no.:	90SB64	90SB67	90SB68	90SB70	90SB72	90SB75	90SB79	93SOB198	93SOB205	93SOB206	93SOB208	93SOB209	93SOB210
Th	9·91	7·23	13·25	4·64	—	—	15·80	9·02	6·74	11·34	11·50	7·08	8·91
U	1·97	1·80	2·12	1·34	—	—	4·71	2·28	1·62	2·15	2·84	1·66	2·09
V	462	389	365	223	331	101	740	321	238	194	254	251	223
Y	34	39	36	29	36	40	42	33	33	35	31	31	40
Zn	113	111	116	87	86	182	141	104	113	109	100	96	112
Zr	390	362	464	440	570	880	485	332	287	381	454	328	472
La	81	91	102	119	—	—	128	79	55	80	96	72	92
Ce	167	212	203	203	—	—	242	156	111	153	186	148	186
Pr	20·76	—	21·95	—	—	—	25·47	17·02	12·58	18·23	—	16·36	20·76
Nd	82	121	94	141	—	—	106	73	56	72	84	71	91
Sm	14·38	16·14	15·65	14·25	—	—	17·62	12·78	11·08	12·81	13·25	12·19	15·77
Eu	4·18	3·86	4·54	4·84	—	—	5·30	3·84	3·44	3·71	4·20	3·72	4·68
Gd	12·00	7·43	12·74	7·30	—	—	15·04	10·89	10·41	10·98	13·25	10·58	13·43
Tb	1·48	1·50	1·59	0·99	—	—	1·81	1·37	1·36	1·43	1·44	1·32	1·70
Dy	7·31	—	7·64	—	—	—	8·71	6·74	6·87	7·09	—	6·44	8·23
Ho	1·22	—	1·27	—	—	—	1·42	1·15	1·17	1·22	1·32	1·10	1·39
Er	2·91	—	3·00	—	—	—	3·36	2·77	2·79	2·97	—	2·60	3·32
Tm	0·39	—	0·41	—	—	—	0·45	0·37	0·38	0·42	—	0·35	0·46
Yb	2·16	2·29	2·25	2·68	—	—	2·47	2·09	2·12	2·39	2·64	1·97	2·56
Lu	0·32	0·27	0·32	0·30	—	—	0·34	0·30	0·30	0·34	0·35	0·29	0·38
$^{87}Sr/^{86}Sr_m$	0·70490	0·70488	0·70500	—	—	—	0·70443	0·70468	0·70431	—	0·70483	0·70451	0·70469
$^{143}Nd/^{144}Nd_m$	0·51248	0·51250	0·51250	—	—	—	0·51256	0·51248	0·51261	—	0·51254	0·51257	0·51260
$^{87}Sr/^{86}Sr_i$	0·70474	0·70484	0·70487	—	—	—	0·70412	0·70450	0·70415	—	0·70472	0·70433	0·70455
$^{143}Nd/^{144}Nd_i$	0·51243	0·51246	0·51245	—	—	—	0·51251	0·51243	0·51254	—	0·51249	0·51251	0·51254
ε_{Nd}	−2·14	−1·43	−1·76	—	—	—	−0·47	−2·16	0·16	—	−0·90	−0·48	0·11

	Main WNW–ESE trend of Serra do Mar igneous centres												
Locality:	Campos do Jordão	Campos do Jordão	Itatiaia (Passa Quatro)	Itatiaia (Passa Quatro)	Itatiaia (Passa Quatro)	Itatiaia	Itatiaia	Itatiaia	Mendanha (Sentíssimo)	Mendanha (Sentíssimo)	Mendanha (Sentíssimo)	Mendanha (Sentíssimo)	Mendanha (Bangu)
Occurrence:	Dyke	Dyke	Dyke	Dyke	Dyke	Dyke	Dyke	Dyke	Dyke	Dyke	Dyke	Dyke	Dyke
Sample no.:	93SOB212	93SOB213	94SOB90	94SOB91	94SOB92	94SOB95	94SOB97	94SOB98	94SOB57	94SOB58	94SOB61	94SOB64	94SOB66
SiO_2	41·42	41·04	46·78	39·47	40·00	46·00	41·21	43·39	43·63	46·72	43·59	44·78	45·54
TiO_2	4·08	4·21	2·92	5·20	4·34	2·59	4·79	4·06	3·53	2·82	3·56	1·84	2·31
Al_2O_3	13·57	13·92	14·52	12·73	10·37	14·55	14·15	12·86	14·19	15·15	14·59	12·90	13·41
Fe_2O_3*	14·42	14·79	10·96	15·80	14·75	10·81	15·26	12·00	11·74	9·97	11·75	11·17	10·38
MnO	0·19	0·19	0·17	0·22	0·20	0·18	0·23	0·19	0·19	0·17	0·20	0·18	0·16
MgO	8·38	7·16	6·70	6·62	10·57	7·90	6·31	6·52	6·56	6·96	6·23	14·64	11·86
CaO	11·35	11·44	9·14	12·12	13·39	9·26	11·09	10·46	10·97	9·46	11·20	10·47	11·74
Na_2O	2·70	3·07	5·00	3·29	2·00	4·65	4·27	3·56	3·20	3·92	3·17	1·81	3·11
K_2O	2·51	2·72	3·19	2·86	2·11	1·95	1·41	4·66	3·49	3·23	3·60	2·04	1·32
P_2O_5	1·06	1·13	0·83	1·98	1·40	0·98	1·05	1·38	1·24	0·85	1·28	0·47	0·60
Total	99·68	99·78	100·21	100·29	99·13	98·87	99·76	99·08	98·75	99·25	99·17	100·30	100·43
LOI	4·88	5·15	5·89	6·84	4·42	1·24	2·72	6·46	3·44	3·88	3·37	6·88	4·45
Ba	1053	1038	1238	964	849	1355	1026	1367	1623	1540	1515	1522	1136
Cr	201	169	226	58	332	187	5	226	205	295	180	752	540
Cs	—	—	—	—	—	0·78	4·66	4·06	2·04	1·87	1·90	7·54	9·03
Cu	46	45	24	37	34	63	30	51	39	32	42	47	48
Ga	20	21	20	18	25	18	24	21	18	18	18	15	16
Hf	7·32	7·22	—	—	7·10	6·55	8·70	10·41	6·08	6·13	6·02	3·83	5·39
Nb	74	85	79	59	55	108	105	154	99	99	98	96	77
Ni	106	77	64	37	141	118	31	61	62	83	53	310	234
Pb	—	—	—	—	—	5·99	6·19	8·82	5·70	6·82	5·86	4·61	5·62
Rb	68	71	97	68	54	41	66	99	92	80	93	138	32
Sc	20	23	20	24	22	18	20	19	21	15	21	23	27
Sr	1253	1280	1104	1055	886	1638	1236	1960	1720	1562	1960	639	771
Ta	5·16	5·64	—	—	3·55	6·69	6·28	9·70	6·49	6·67	6·36	5·50	4·45

Table 2: continued

	Main WNW–ESE trend of Serra do Mar igneous centres												
Locality:	Campos do Jordão	Campos do Jordão	Itatiaia (Passa Quatro)	Itatiaia (Passa Quatro)	Itatiaia (Passa Quatro)	Itatiaia	Itatiaia	Itatiaia	Mendanha (Sentíssimo)	Mendanha (Sentíssimo)	Mendanha (Sentíssimo)	Mendanha (Sentíssimo)	Mendanha (Bangu)
Occurrence:	Dyke	Dyke	Dyke	Dyke	Dyke	Dyke	Dyke	Dyke	Dyke	Dyke	Dyke	Dyke	Dyke
Sample no.:	93SOB212	93SOB213	94SOB90	94SOB91	94SOB92	94SOB95	94SOB97	94SOB98	94SOB57	94SOB58	94SOB61	94SOB64	94SOB66
Th	8·40	8·99	—	—	6·36	7·92	9·10	12·11	6·13	7·09	6·22	5·87	4·97
U	1·86	2·04	—	—	1·16	1·98	2·16	2·87	1·37	1·59	1·38	1·13	1·03
V	316	325	228	350	314	198	350	279	257	203	252	214	239
Y	33	31	29	39	33	35	38	40	36	31	35	21	25
Zn	97	103	114	95	84	89	120	102	94	81	93	82	75
Zr	344	340	349	377	264	282	361	450	246	259	241	166	219
La	75	84	—	—	74	104	88	137	76	68	75	54	43
Ce	146	167	—	—	142	180	176	237	161	139	149	99	83
Pr	—	—	—	—	—	23·37	21·91	33·89	21·26	17·79	20·99	11·26	10·04
Nd	69	76	—	—	71	88	87	126	87	71	87	42	40
Sm	11·64	12·61	—	—	12·50	13·55	15·24	19·29	14·89	12·01	14·80	6·74	7·44
Eu	3·17	3·97	—	—	3·31	4·00	4·45	5·39	4·60	3·78	4·55	2·12	2·33
Gd	56·25	14·68	—	—	—	11·36	12·54	15·41	12·47	10·01	12·01	6·13	6·74
Tb	1·34	1·08	—	—	1·32	1·39	1·60	1·80	1·54	1·27	1·49	0·77	0·92
Dy	—	—	—	—	—	6·96	7·87	8·62	7·57	6·45	7·36	3·93	4·91
Ho	1·18	1·07	—	—	0·86	1·24	1·33	1·41	1·27	1·09	1·26	0·73	0·89
Er	—	—	—	—	—	3·13	3·12	3·40	3·06	2·68	3·00	1·84	2·20
Tm	—	—	—	—	—	0·46	0·44	0·46	0·42	0·38	0·41	0·27	0·33
Yb	2·16	2·45	—	—	1·98	2·61	2·43	2·51	2·33	2·11	2·91	1·56	1·87
Lu	0·38	0·31	—	—	0·24	0·39	0·34	0·35	0·34	0·31	0·33	0·24	0·28
$^{87}Sr/^{86}Sr_m$	0·70458	0·70467	—	—	—	0·70503	0·70470	0·70535	0·70471	0·70485	—	0·70884	0·70497
$^{143}Nd/^{144}Nd_m$	0·51255	0·51251	—	—	—	0·51242	0·51256	0·51242	0·51256	0·51255	—	0·51257	0·51260
$^{87}Sr/^{86}Sr_i$	0·70440	0·70448	—	—	—	0·70495	0·70453	0·70519	0·70455	0·70470	—	0·70820	0·70485
$^{143}Nd/^{144}Nd_i$	0·51250	0·51245	—	—	—	0·51237	0·51251	0·51237	0·51251	0·51250	—	0·51252	0·51255
ε_{Nd}	−0·78	−1·62	—	—	—	−3·24	−0·66	−3·29	−0·61	−0·85	—	−0·46	−0·07

	Main WNW–ESE trend of Serra do Mar igneous centres												
Locality:	Mendanha (Bangu)	Mendanha (Realengo)	Mendanha (Nova Iguaçu)	Mendanha (Nova Iguaçu)	Mendanha (Nova Iguaçu)	São José do Itaboraí	São José do Itaboraí	Soarinho	Soarinho	Soarinho	Morro de São João	Cabo Frio	Cabo Frio
Occurrence:	Dyke	Dyke	Dyke	Dyke	Dyke	Lava	Lava	Dyke	Dyke	Dyke	Syenite	Dyke	Dyke
Sample no.:	94SOB67	94SOB68	94SOB78	94SOB80	94SOB81	94SOB50	94SOB51	94SOB127	94SOB128	94SOB131	94SOB142	93SOB191	93SOB193
SiO_2	45·28	44·52	48·70	46·78	43·97	42·85	42·83	48·00	49·02	37·23	46·13	51·76	46·53
TiO_2	2·38	2·88	2·51	2·92	4·10	3·68	3·69	3·04	2·76	6·20	3·47	1·14	2·23
Al_2O_3	12·80	16·26	15·08	14·52	15·75	13·39	13·45	16·12	16·51	11·61	16·31	19·72	14·25
Fe_2O_3*	10·49	11·31	10·29	10·96	11·51	11·50	12·36	9·95	9·00	15·76	9·90	5·88	10·41
MnO	0·17	0·19	0·18	0·17	0·22	0·22	0·21	0·17	0·16	0·22	0·24	0·19	0·17
MgO	12·29	5·69	5·30	6·70	4·38	8·41	7·78	3·18	3·95	6·88	3·33	2·11	8·34
CaO	12·19	10·29	8·11	9·14	9·54	13·98	14·50	7·39	7·37	13·52	8·87	4·46	12·10
Na_2O	2·80	3·57	4·74	5·00	3·60	3·19	2·67	1·34	1·60	1·01	2·31	7·63	2·98
K_2O	0·94	3·52	3·53	3·19	4·44	0·75	0·65	7·94	6·99	3·46	7·21	5·96	2·46
P_2O_5	0·57	0·87	0·92	0·83	1·34	1·39	1·38	0·92	0·84	2·32	1·03	0·32	0·51
Total	99·91	99·10	99·35	100·21	98·85	99·36	99·51	98·95	99·01	99·08	99·37	99·22	99·98
LOI	4·10	4·02	3·76	3·10	5·20	4·04	4·56	9·31	9·17	8·56	0·87	3·00	3·89
Ba	1132	1338	1628	1634	2436	1713	2026	2696	2704	3580	894	441	1047
Cr	549	73	216	136	2	304	295	119	113	10	6	3	313
Cs	12·59	4·70	2·64	1·79	—	—	—	10·74	—	7·14	2·66	—	—
Cu	51	38	29	52	16	31	29	1	8	22	19	17	58
Ga	16	20	19	18	15	16	13	18	16	17	20	20	19
Hf	5·52	5·22	6·63	4·73	—	4·96	—	8·55	—	7·20	9·14	—	4·76
Nb	73	173	80	58	67	88	59	149	101	71	111	195	63
Ni	252	41	56	72	14	159	124	38	37	33	9	11	105
Pb	5·49	5·84	7·75	3·65	—	2·83		7·70	—	3·97	4·78	—	—
Rb	34	96	93	78	132	31	40	164	150	89	252	177	48
Sc	28	18	18	31	15	23	24	10	13	24	11	5	25
Sr	803	1234	1189	1286	2012	2174	2158	5166	5331	5542	2176	468	1098
Ta	4·58	11·23	4·81	3·67	—	4·88	—	11·29	—	4·96	5·93	—	4·15

Table 2: continued

	Main WNW–ESE trend of Serra do Mar igneous centres												
Locality:	Mendanha (Bangu)	Mendanha (Realengo)	Mendanha (Nova Iguaçu)	Mendanha (Nova Iguaçu)	Mendanha (Nova Iguaçu)	São José do Itaboraí	São José do Itaboraí	Soarinho	Soarinho	Soarinho	Morro de São João	Cabo Frio	Cabo Frio
Occurrence:	Dyke	Dyke	Dyke	Dyke	Dyke	Lava	Lava	Dyke	Dyke	Dyke	Syenite	Dyke	Dyke
Sample no.:	94SOB67	94SOB68	94SOB78	94SOB80	94SOB81	94SOB50	94SOB51	94SOB127	94SOB128	94SOB131	94SOB142	93SOB191	93SOB193
Th	4·74	8·41	7·10	4·18	—	4·56	—	9·55	—	5·54	8·53	—	7·06
U	1·00	1·47	1·56	0·94	—	0·91	—	1·85	—	1·18	1·80	—	1·38
V	234	243	181	371	272	310	305	93	94	331	183	114	251
Y	25	28	28	30	41	37	28	41	44	43	40	27	25
Zn	78	88	105	93	109	96	89	92	96	115	107	98	69
Zr	218	219	286	186	291	199	200	366	394	253	383	706	201
La	41	81	73	58	—	83	—	142	—	84	125	—	62
Ce	80	148	146	124	—	161	—	247	—	178	202	—	115
Pr	9·73	17·17	17·75	16·60	—	21·96	—	35·89	—	28·81	26·47	—	—
Nd	39	63	69	70	—	88	—	133	—	131	98	—	51
Sm	7·37	9·93	11·05	12·19	—	14·41	—	19·39	—	24·14	15·11	—	7·85
Eu	2·32	2·98	3·53	4·05	—	4·62	—	6·14	—	7·73	4·29	—	2·18
Gd	6·81	8·15	9·07	10·32	—	12·04	—	15·14	—	19·03	12·45	—	38·74
Tb	0·92	1·04	1·12	1·28	—	1·48	—	1·81	—	2·26	1·56	—	0·98
Dy	4·88	5·39	5·63	6·25	—	7·45	—	8·87	—	10·55	7·90	—	—
Ho	0·87	0·97	0·98	1·08	—	1·28	—	1·48	—	1·70	1·39	—	1·02
Er	2·20	2·51	2·43	2·57	—	3·10	—	3·51	—	3·75	3·54	—	—
Tm	0·33	0·37	0·35	0·36	—	0·44	—	0·48	—	0·46	0·51	—	—
Yb	1·86	2·16	1·99	1·95	—	2·39	—	2·59	—	2·44	2·91	—	2·22
Lu	0·28	0·33	0·29	0·28	—	0·35	—	0·36	—	0·33	0·45	—	0·28
$^{87}Sr/^{86}Sr_m$	—	—	—	—	—	0·70459	—	0·70492	—	0·70498	—	—	0·70434
$^{143}Nd/^{144}Nd_m$	—	—	—	—	—	0·51249	—	0·51251	—	0·51246	—	—	0·51250
$^{87}Sr/^{86}Sr_i$	—	—	—	—	—	0·70455	—	0·70484	—	0·70494	—	—	0·70425
$^{143}Nd/^{144}Nd_i$	—	—	—	—	—	0·51245	—	0·51247	—	0·51241	—	—	0·51247
ε_{Nd}	—	—	—	—	—	−2·00	—	−1·60	—	−2·86	—	—	−1·90

	Offshore islands and adjacent coast										Neogene localities		
Locality:	Cabo Frio	Cabo Frio	Trigo	Trigo	Trigo	São Sebastião	São Sebastião	São Sebastião	Ilhabela	Ilhabela	Estrada do Grumari	Fazenda Modelo	Volta Redonda
Occurrence:	Dyke	Dyke	Dyke	Dyke	Dyke	Dyke	Dyke	Dyke	Dyke	Dyke	Dyke	Dyke	Lava
Sample no.:	93SOB196	93SOB197	94SOB14	94SOB17	94SOB20	94SOB10	94SOB12	94SOB13	90SB54	94SOB31	94SOB55	94SOB56	94SOB89
SiO_2	42·55	44·42	40·71	43·94	40·89	41·14	42·24	42·86	40·77	44·55	45·07	44·06	45·17
TiO_2	2·84	3·31	4·32	2·54	3·01	2·46	1·97	1·97	2·24	2·53	2·36	2·21	2·41
Al_2O_3	14·62	14·05	13·84	13·39	13·08	12·29	14·74	11·57	11·76	11·59	12·63	13·38	14·22
Fe_2O_3*	12·37	12·82	15·38	12·47	15·10	12·67	12·57	11·56	12·59	12·38	11·26	10·72	11·07
MnO	0·22	0·17	0·17	0·20	0·24	0·21	0·20	0·16	0·21	0·18	0·18	0·18	0·19
MgO	6·02	7·21	7·01	10·02	8·54	9·09	7·54	16·43	10·03	11·08	13·03	13·99	10·96
CaO	12·02	10·48	10·74	12·19	11·90	16·97	14·54	12·68	17·10	14·49	10·40	10·61	10·65
Na_2O	2·09	2·83	3·86	2·60	2·61	1·72	2·03	0·65	1·87	1·62	3·33	3·32	3·75
K_2O	5·16	2·66	1·85	1·78	1·34	1·69	1·95	1·51	1·46	1·45	1·27	1·45	0·96
P_2O_5	0·92	1·35	0·76	0·94	1·38	0·93	1·28	0·61	0·98	0·36	0·77	0·68	0·91
Total	98·93	99·48	98·76	100·07	98·29	99·37	99·24	100·00	99·01	100·23	100·29	100·60	100·29
LOI	7·19	5·01	1·74	0·21	0·35	5·43	5·31	7·97	2·87	0·25	1·34	1·31	3·10
Ba	1351	1802	502	615	664	732	643	1477	624	501	1094	1029	1106
Cr	30	134	87	309	170	333	28	1066	334	483	744	707	236
Cs	—	—	1·55	0·74	0·30	1·40	1·80	2·10	—	2·08	0·82	0·78	1·10
Cu	48	32	46	43	109	97	90	71	—	72	49	49	38
Ga	19	18	23	19	22	18	18	14	15	17	17	16	17
Hf	8·40	6·40	5·67	5·66	5·37	5·17	5·14	4·12	5·89	5·14	5·34	4·94	5·07
Nb	133	81	48	72	93	82	57	58	49	55	77	70	85
Ni	30	71	86	174	138	143	122	460	177	191	380	347	177
Pb	—	—	9·78	3·43	2·58	4·34	3·82	3·02	—	5·44	4·27	4·04	4·08
Rb	113	31	44	54	26	46	47	62	32	46	26	42	35
Sc	23	23	20	21	13	23	16	34	33	38	23	24	23
Sr	1732	2213	754	1093	1503	1250	1144	656	1154	643	1158	916	1021
Ta	6·85	5·62	3·06	7·44	9·11	6·76	3·41	3·74	3·36	3·29	4·65	4·13	4·92

Table 2: continued

	Offshore islands and adjacent coast										Neogene localities		
Locality:	Cabo Frio	Cabo Frio	Trigo	Trigo	Trigo	São Sebastião	São Sebastião	São Sebastião	Ilhabela	Ilhabela	Estrada do Grumari	Fazenda Modelo	Volta Redonda
Occurrence:	Dyke	Dyke	Dyke	Dyke	Dyke	Dyke	Dyke	Dyke	Dyke	Dyke	Dyke	Dyke	Lava
Sample no.:	93SOB196	93SOB197	94SOB14	94SOB17	94SOB20	94SOB10	94SOB12	94SOB13	90SB54	94SOB31	94SOB55	94SOB56	94SOB89
Th	15·17	6·68	4·30	4·64	2·71	7·01	6·90	4·37	4·99	3·60	6·49	5·43	6·63
U	3·09	1·28	1·26	4·53	2·95	5·15	2·54	1·41	2·48	0·95	1·42	1·25	1·67
V	283	233	367	246	265	322	260	257	305	398	215	224	201
Y	33	35	32	33	37	28	36	22	31	24	28	27	28
Zn	88	109	141	100	131	99	97	83	67	94	81	88	82
Zr	336	228	223	256	260	245	270	180	257	189	229	214	224
La	122	111	45	61	75	68	67	43	57	38	58	49	60
Ce	230	222	97	125	152	136	134	85	127	80	114	97	114
Pr	—	—	12·78	15·42	16·72	14·83	14·64	10·19	—	10·40	14·08	12·10	13·63
Nd	94	113	56	62	72	64	64	40	59	43	56	49	54
Sm	13·78	17·29	11·86	11·17	12·94	11·24	11·28	7·34	10·84	8·20	9·94	8·78	9·45
Eu	3·98	5·49	3·50	3·39	3·99	3·34	3·39	2·36	3·34	2·49	3·11	2·80	2·98
Gd	11·03	14·03	10·66	9·63	11·87	9·52	10·16	6·64	6·20	7·16	8·75	7·87	8·10
Tb	1·28	1·69	1·42	1·29	1·54	1·21	1·33	0·84	1·38	0·96	1·11	1·02	1·08
Dy	—		7·03	6·61	7·74	5·97	7·01	4·38	—	4·91	5·65	5·19	5·63
Ho	1·21	1·45	1·16	1·16	1·34	1·01	1·25	0·78	1·07	0·85	0·98	0·92	0·99
Er	—		2·64	2·81	3·32	2·47	3·19	1·69	—	2·08	2·45	2·31	2·48
Tm	—		0·34	0·40	0·45	0·33	0·46	0·29	—	0·29	0·35	0·33	0·35
Yb	2·80	3·44	1·85	2·24	2·58	1·86	2·74	1·65	2·27	1·65	2·00	1·91	2·02
Lu	0·31	0·40	0·26	0·32	0·38	0·28	0·40	0·25	0·32	0·24	0·29	0·28	0·30
$^{87}Sr/^{86}Sr_m$	0·70419	0·70463	0·70428	0·70405	0·70404	0·70453	0·70433	0·70692	0·70441	0·70459	0·70443	0·70433	0·70397
$^{143}Nd/^{144}Nd_m$	0·51244	0·51242	0·51261	0·51273	0·51268	0·51270	0·51272	0·51269	0·51272	0·51262	0·51255	0·51256	0·51259
$^{87}Sr/^{86}Sr_i$	0·70404	0·70460	0·70409	0·70389	0·70399	0·70441	0·70419	0·70661	0·70432	0·70435	0·70441	0·70427	0·70393
$^{143}Nd/^{144}Nd_i$	0·51241	0·51239	0·51254	0·51267	0·51262	0·51264	0·51267	0·51264	0·51266	0·51256	0·51253	0·51253	0·51257
ε_{Nd}	−3·06	−3·56	0·09	2·68	1·75	2·07	2·55	1·96	2·41	0·47	−1·38	−1·26	−0·53

*Total Fe presented as Fe_2O_3.
Major elements presented on a volatile-free basis. All samples were acid-leached before isotopic analysis. $^{87}Sr/^{86}Sr$ and $^{143}Nd/^{144}Nd$ are listed as measured (m) and initial values (i), corrected to dates of emplacement (see Fig. 6). ε_{Nd} was calculated using the same emplacement ages. See Appendix A for sample localities. See Gibson *et al.* (1995) and Appendix B for analytical techniques.

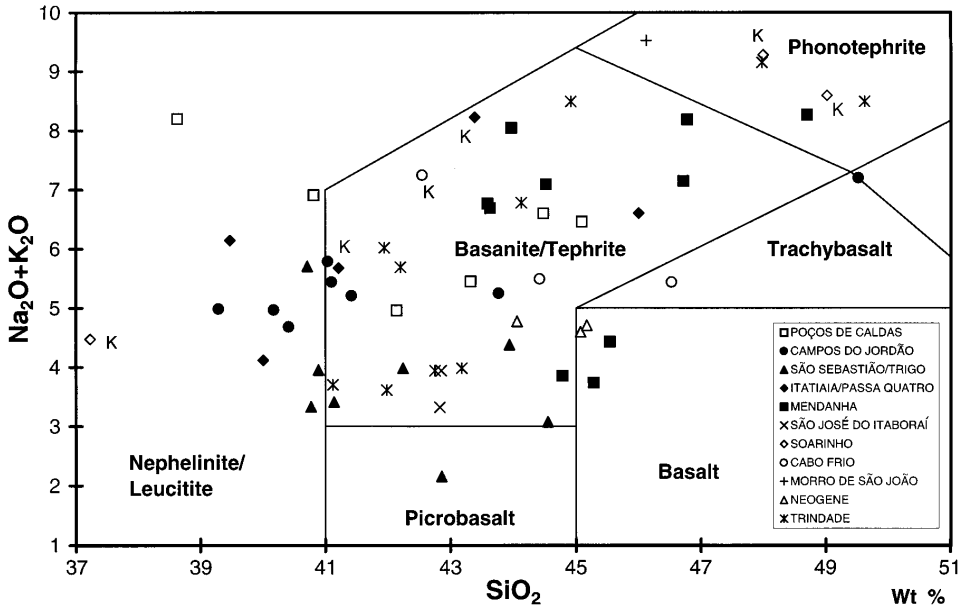

Fig. 7. Variation of total alkalis ($Na_2O + K_2O$) with SiO_2 in igneous rocks from the Serra do Mar province analysed for this research. It should be noted that the predominating syenites of the province are not considered here. TAS subdivisions are from Le Maitre (1989). K identifies samples with phlogopite–biotite phenocrysts. In addition, Poços de Caldas and Morro de São João samples contain leucite (variably altered to analcite). Trindade data are from Halliday *et al.* (1992) and J. C. Greenwood (unpublished data, 1997).

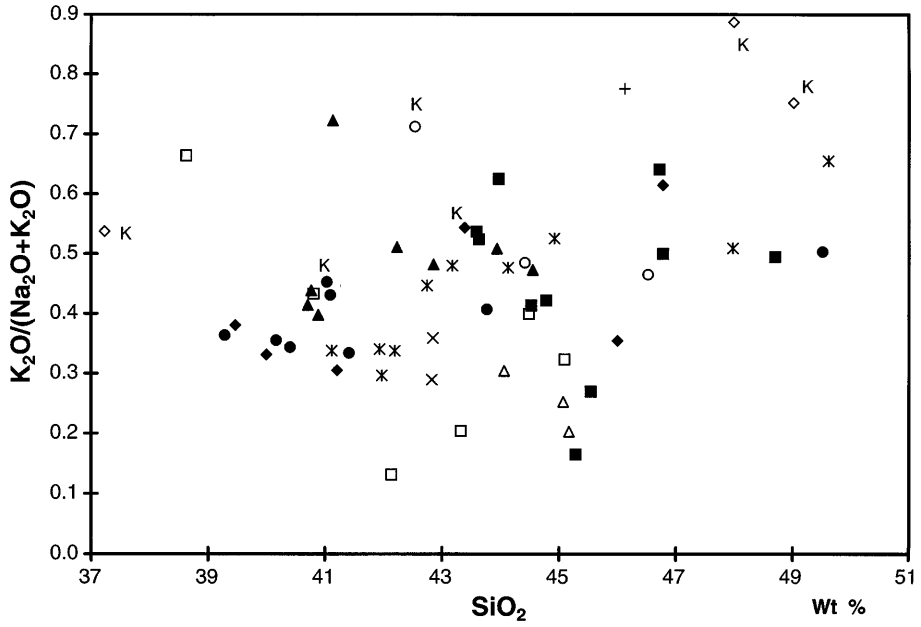

Fig. 8. Variation of $K_2O/(Na_2O + K_2O)$ with SiO_2 in the same Serra do Mar suite as in Fig. 7. (See Fig. 7 for the key to sample localities and other notes.)

Trindade (J. C. Greenwood, unpublished data, 1997) in all plotted elements except K and Rb (sensitive to both alteration and the presence of residual phlogopite in the mantle source) and P (variable from suite to suite in OIBs). Likewise, the patterns of all the more sodic samples (Fig. 8) plotted in Fig. 11 are fundamentally very similar and OIB-like. The relatively low K in sample 94SOB50, from São José do Itaboraí, may be due to the somewhat

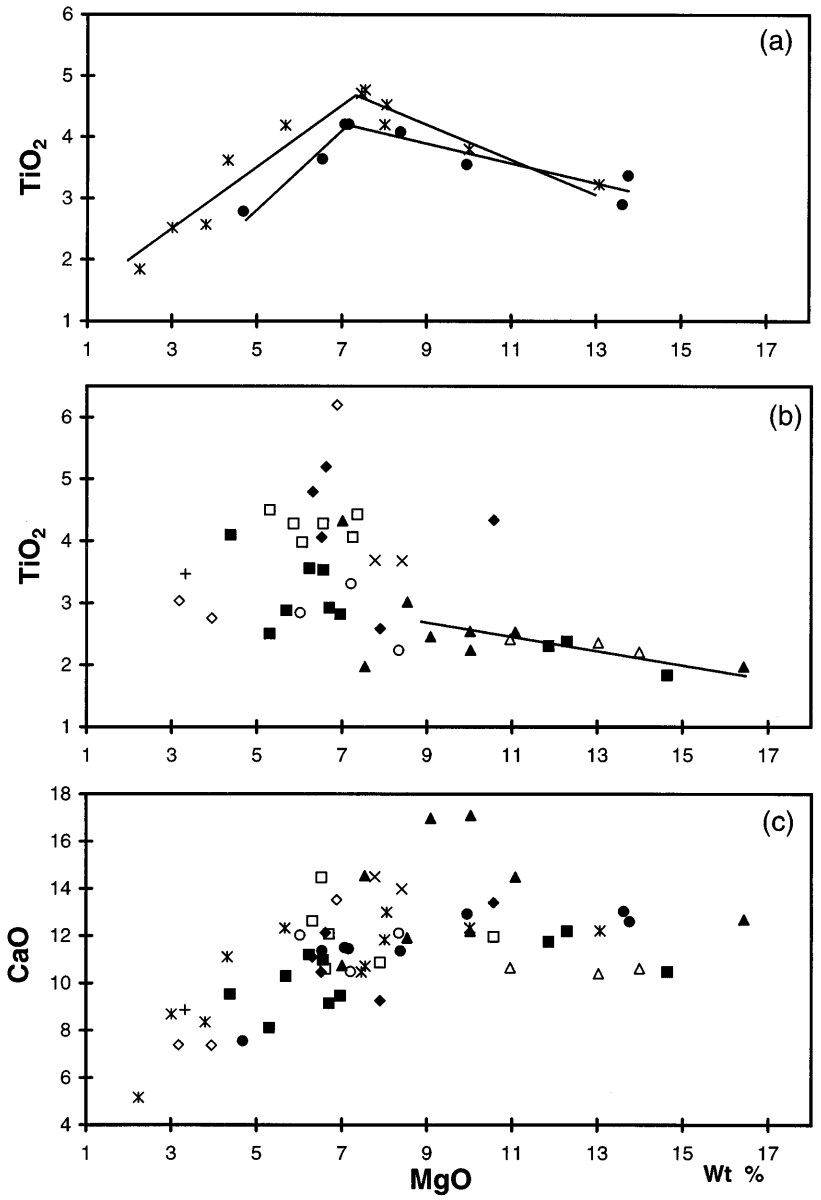

Fig. 9. Variation of TiO_2 and CaO with MgO in the same Serra do Mar suite as in Fig. 7. (See Fig. 7 for the key to sample localities; see text for discussion of the trend-lines.)

altered state of the sample, with chloritized biotite. Most mafic igneous rocks from sub-continental lithospheric mantle sources show 'spiky' patterns in normalized diagrams, such as Fig. 11. The Soarinho minette 94SOB131 has such a pattern but those of the most potassic samples from Itatiaia and Cabo Frio are smooth and OIB-like, resembling the Tristan da Cunha basalt plotted for comparison. To summarize the major- and trace-element compositions of the Serra do Mar mafic rocks: (1) they are mostly basanites to melanephelinites, with occasional more potassic variants; (2) fractional crystallization controlled magmatic evolution within each local suite; (3) the more magnesian samples are all, except one Soarinho minette, closely similar in composition to OIB.

Sr–Nd isotopes

A plot of Sr- and Nd-isotopic ratios (Fig. 12) shows that, apart from two obvious exceptions with very high $^{87}Sr/^{86}Sr$, the Serra do Mar data set forms a scattered trend, between São Sebastião–Trigo samples with $\varepsilon_{Nd} \sim +2{\cdot}5$ and $^{87}Sr/^{86}Sr_i < 0{\cdot}7040$, and samples from Itatiaia–Passa Quatro, Soarinho and Cabo Frio, with $\varepsilon_{Nd} < -2{\cdot}9$ and

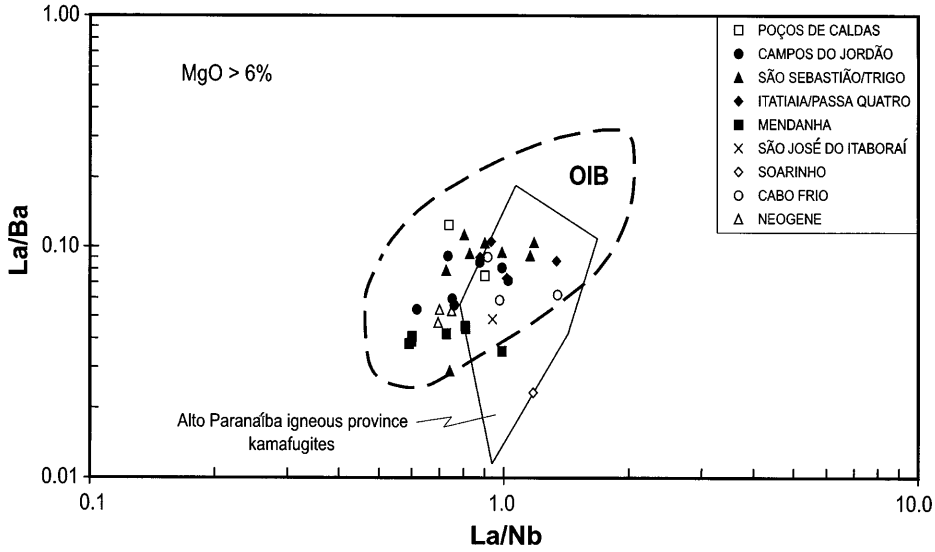

Fig. 10. Variation of La/Ba with La/Nb in Serra do Mar province samples with >6% MgO (Table 1). The field marked OIB encloses basic lavas from oceanic islands distant from subduction zones (Fitton *et al.*, 1991). The field of Alto Paranaíba province kamafugites is from Gibson *et al.* (1995).

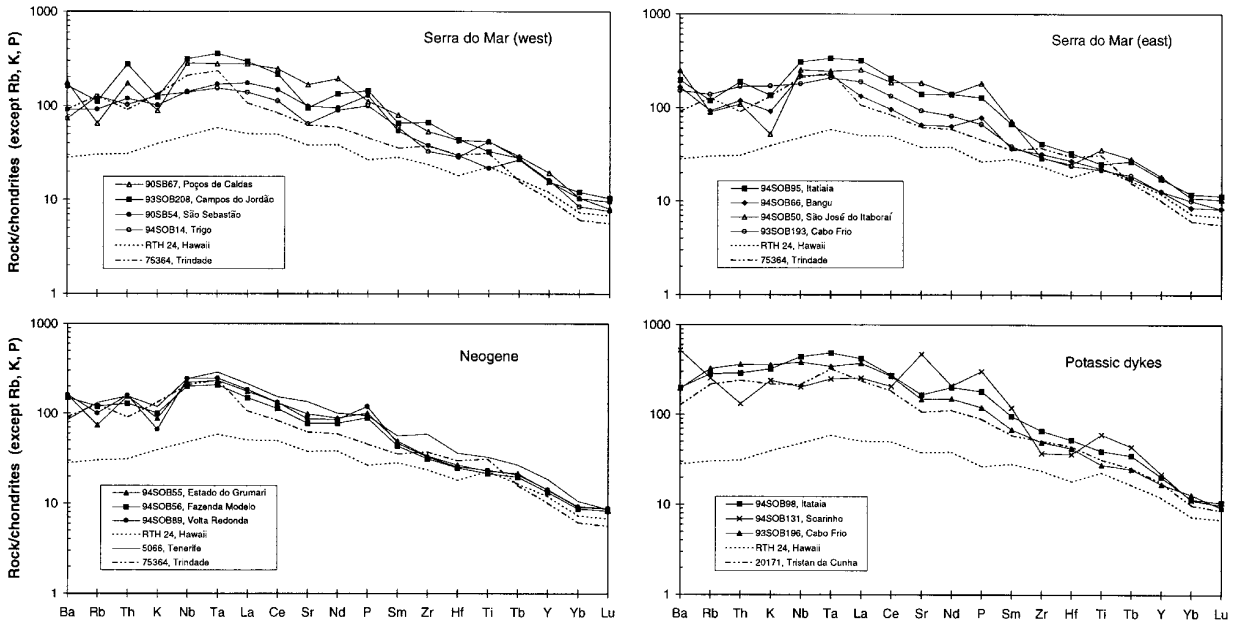

Fig. 11. Normalized multi-element plots of representative mafic rock types from the Serra do Mar igneous province (Table 2). The normalization factors and comparative OIB data are from Thompson *et al.* (1984) and J. C. Greenwood (Trindade; unpublished data, 1997).

$^{87}Sr/^{86}Sr_i$ >0·7046. Three of the five samples with lowest ε_{Nd} values contain phlogopite phenocrysts. In Fig. 12 these lie adjacent to the field of the ~85 Ma Alto Paranaíba mafic ultrapotassic rocks (Gibson *et al.*, 1995) that crop out about 500 km to the northwest (Fig. 1).

Two entirely different models could potentially explain the Serra do Mar Sr–Nd isotopic array:

(1) The samples may define a broad mixing line between an OIB end-member (from convecting mantle sources) that had similar ε_{Nd} values to those of Trindade

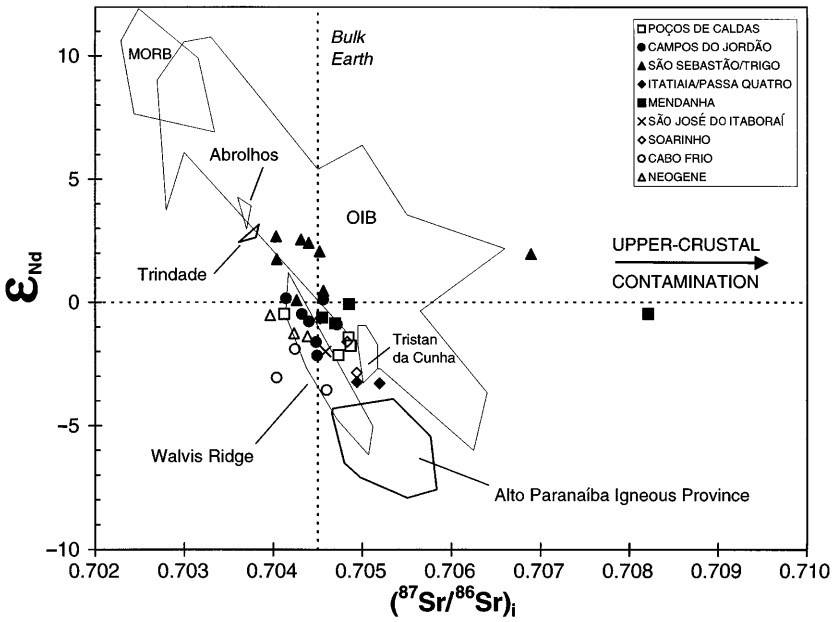

Fig. 12. Initial Sr- and Nd-isotopic ratios in mafic alkaline igneous rocks from the Serra do Mar province. For comparison, the fields are also shown for world-wide MORB and OIB; South Atlantic OIBs close in space and/or time to Serra do Mar; and mafic ultrapotassic rock-types of the Alto Paranaíba igneous province, SE Brazil (Fig. 1). [See Gibson *et al.* (1995, fig. 12) for the sources of published data.]

and the Abrolhos Platform, and a sub-continental lithospheric mantle end-member that isotopically resembled the Alto Paranaíba ultrapotassics.

(2) All the Serra do Mar mafic magmas may come from a range of convecting-mantle sources; the more sodic batches from Trindade-like, OIB-source mantle and the more potassic batches from zones, streaks or blobs that resembled geochemically the sources of the Tristan da Cunha and Walvis Ridge magmatism.

As other studies at this latitude on both sides of the South Atlantic have found, it is extremely difficult to differentiate unequivocally between these two contrasting geochemical models (e.g. Milner & le Roex, 1996; Gibson *et al.*, 1997*b*, 1997*c*). We consider two clues that model 1 may be correct:

(1) The sample with the highest ε_{Nd}, overlapping the Trindade range, comes from Trigo, which is the nearest point in this study to the Brazilian continental margin. Trigo is sited within the Campos basin on strongly attenuated continental lithosphere (Chang *et al.*, 1992); the most sensible place to seek magmas that sampled the subjacent convecting mantle, with minimal subsequent lithospheric input during their uprise. Furthermore, the dykes are late-stage members of the Trigo complex, cutting syenites and layered gabbro. It is probable that any fusible lithospheric components had already been removed, in earlier melt batches, before the magmas of these dykes were generated. A similar explanation applies to the high-ε_{Nd}, post-syenite dykes of Ilhabela (part of the São Sebastião suite).

(2) Most data from individual complexes tend to cluster, rather than to be distributed randomly throughout the array in Fig. 12. This can, of course, be explained within a convecting mantle source framework by postulating distinctive local streaks or blobs beneath each centre. It is the Cabo Frio data that encourage us to think that these local geochemical characteristics were within the lithosphere, rather than beneath it. The Cabo Frio points all lie to the left of the main Serra do Mar array. Furthermore, one of them, minette 93SOB196, lies well outside the field of all known OIBs in Fig. 12. If the Cabo Frio samples contain a substantial lithospheric component, it appears to be EM1-like (Hofmann, 1997) and might therefore reside in the lithospheric mantle root of an Archaean craton or platform (Menzies, 1989). This suggestion is consistent with the independent evidence of Fonseca *et al.* (1995) that the Cabo Frio area differs from the rest of SE Brazil in preserving a reworked fragment of the Congo–Kasai craton (Fig. 1, inset).

We therefore conclude that the available data favour the view that all but the two high-$^{87}Sr/^{86}Sr_i$ Serra do Mar samples are mixtures of melts from both convecting (predominantly) and lithospheric mantle sources, with the latter varying locally but overall resembling the sources of the Alto Paranaíba mafic ultrapotassic magmas. We appreciate that our data do not yet exclude a variable

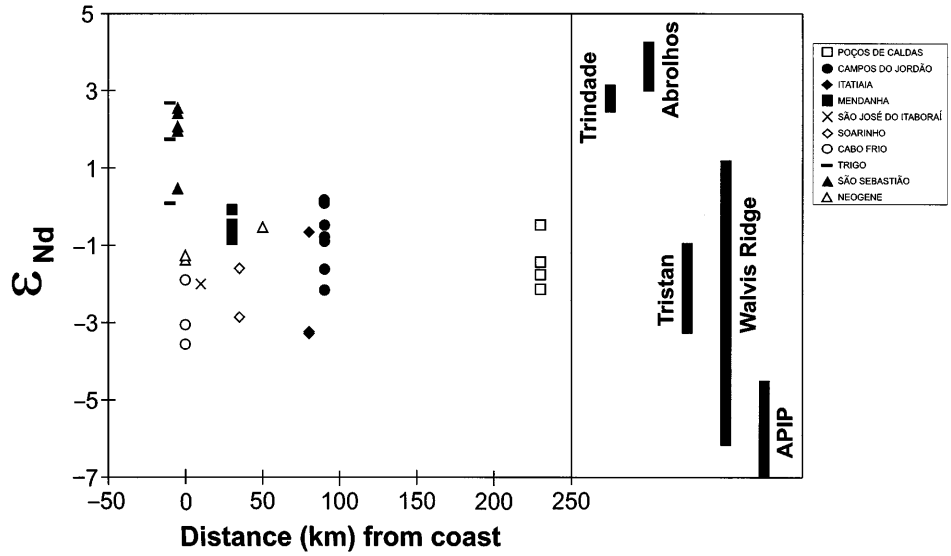

Fig. 13. The ε_{Nd} values of Serra do Mar province mafic igneous rocks plotted as a function of the distance between each igneous centre and the present-day coast. This approximately reflects distance from the continental margin. The ε_{Nd} ranges of relevant South Atlantic OIBs and late Cretaceous mafic ultrapotassic rock-types of the Alto Paranaíba igneous province (APIP; Fig. 1) are given for comparison. (See Fig. 12 for data sources.)

convecting mantle source hypothesis and we aim to test these alternatives by Os-isotope studies (J. C. Greenwood, work in progress).

Crustal (ATA) contamination of two picrites

The two samples with very high $^{87}Sr/^{86}Sr_i$—picrites from São Sebastião (94SOB13) and Sentísssimo, Mendanha, (94SOB64)—have the two highest MgO contents (Table 2). Despite high $^{87}Sr/^{86}Sr_i$, their ε_{Nd} values are within the range of other samples from the same locality. This is particularly clear for the Mendanha set (Table 2; Figs 12 and 13). An input from selectively dissolved crustal K-feldspar would explain the isotope systematics. Is this realistic for dykes? Sample 94SOB64 is ~30 cm thick and 94SOB13 is only 10 cm thick at its maximum. Both are emplaced into granitic gneisses.

There is theoretical, observational and geochemical evidence that MgO-rich liquids with low viscosities can flow turbulently within the crust and hence become very rapidly contaminated by fusible components of their wallrocks (Moorbath & Thompson, 1980; Huppert & Sparks, 1985; Kille *et al.*, 1986). Kerr *et al.* (1995) proposed that this process should be called Assimilation during Turbulent magma Ascent (ATA), to contrast it with the well-known AFC (assimilation–fractional crystallization) process. The transition between turbulent and laminar flow in a liquid is abrupt (e.g. Huppert & Sparks, 1985) and therefore it is possible that the two most MgO-rich dykes could become contaminated, whereas all the others escaped unaffected. But even less MgO-rich, more viscous basic liquids will sometimes locally flow turbulently in dykes, as they pass obstructions (Kille *et al.*, 1986), and therefore they too can become affected by ATA contamination. This may be the reason why the high-ε_{Nd} São Sebastão–Trigo samples in Fig. 12 show a spread of $^{87}Sr/^{86}Sr_i$, even when 94SOB13 is excluded, and all plot at higher $^{87}Sr/^{86}Sr_i$ values than the Trindade field. We have emphasized this evidence for crustal contamination because most investigators of small-volume mafic magmatism tend to dismiss it (e.g. Comin-Chiaramonti *et al.*, 1997). If some or most of these scattered dykes and small lavas have dissolved crust, the detailed geochemical modelling of their genesis and subsequent evolution becomes very difficult. Such modelling requires isotopic analyses of the more evolved rock-types, as is being undertaken by others (e.g. Valente *et al.*, 1995).

It is implicit in the foregoing discussion that the ε_{Nd} values of the Serra do Mar mafic rocks seem to be essentially unaffected by any postulated crustal contamination. Figure 13 shows that the ε_{Nd} ranges of most Serra do Mar suites are fairly large. Despite the point we made above about the offshore island of Trigo producing our highest-ε_{Nd} sample, it is clear from Fig. 13 that there is no sign of a progressive reduction in ε_{Nd} away from the continental margin; the entire ε_{Nd} range occurs in complexes along or adjacent to the present coastline. This reinforces the view that a significant factor in allowing high-ε_{Nd} magmas to reach the upper crust at Trigo and São Sebastião was their late genesis in the local magmatic sequences.

DISCUSSION

Serra do Mar province mafic magma sources

In the previous section we have argued that the geochemistry of the Serra do Mar mafic magmas is best explained by a model in which their ultimate source was predominantly within the convecting mantle but that, during their uprise, individual magma batches:

(1) mixed to varying extents with diverse melts from fusible metasomites within the sub-continental lithospheric mantle;

(2) assimilated fusible crustal rock-types but only did so extensively in the rare cases when MgO-rich magma batches flowed turbulently during their emplacement;

(3) underwent varying amounts of fractional crystallization.

The first two of these processes can substantially affect both the abundances and ratios of rare earth elements (REE) and other incompatible elements in mafic magmas. For this reason it is inappropriate, in this case, to use REE inversion calculations (McKenzie & O'Nions, 1991, 1995) to define further the convecting-mantle sources and melting conditions of the magmas. Nevertheless, the high-ε_{Nd} São Sebastão–Trigo basanites and nephelinites (Fig. 7) should yield defensible REE-inversion results.

To model the genesis of the Serra do Mar initial magmas in a simple way, without over-interpreting the data, we have used the approach of Kostopoulos & James (1992), derived from the non-modal batch melting equations of Shaw (1979). Figure 14 shows arrays of calculated small-degree melt compositions for anhydrous fusion of lherzolite mantle at depths where spinel or garnet, or a 50:50 mixture of the two, is the fourth phase. The arrays are calculated for two contrasting hypothetical variants of lherzolite: DMM (Depleted MORB-source Mantle) and BSE (Bulk Silicate Earth), as defined by Kostopoulos & James (1992). These lherzolite variants are very similar to the hypothetical 'MORB-source' and 'primitive' mantles used by McKenzie & O'Nions (1991, 1995). It is clear from Fig. 12 that, taking the Serra do Mar data set as a whole, its time-integrated values of Rb/Sr and Sm/Nd are close to those defined for BSE melts, and that the BSE array in Fig. 14 is therefore appropriate. Of course, the situation is different if one accepts the arguments that we made in the last section, that only the Serra do Mar melts with the highest ε_{Nd} values should be modelled as simple one-stage melts of convecting mantle, free from low-ε_{Nd} post-genesis inputs. In the latter case, the logical array to calculate and plot in Fig. 14 is the set of melts from an ~50:50 mixture of DMM and BSE because this would generate time-integrated values of Rb/Sr and Sm/Nd similar to those of the Trindade lavas. This is close to the mantle source calculated by Gibson *et al.* (1997*c*), using inversion modelling, for the OIB-like alkali basalts emplaced at ~84 Ma above the Trindade mantle plume head at Poxoréu, Mato Grosso, in central Brazil.

Only REE determined by ICP-MS are plotted in Fig. 14. As a group, the Serra do Mar mafic magmas may be interpreted in terms of ~0·1–1·0% melts of a BSE lherzolite mantle, with a garnet:spinel ratio around 70:30. It is clear from the diagram that, if the chosen mantle source was instead a 50:50 mixture of BSE and DMM, the degrees of melting indicated would be smaller but the estimated garnet:spinel ratio of the source would not change greatly. Conversely, there is ample petrographic evidence (see above) that these magmas were relatively volatile rich; a factor that would increase the estimated degrees of melting (Hirose & Kawamoto, 1995). McKenzie (1989) has emphasized the ease with which very small fractions of low-viscosity, picritic, volatile-rich, mafic alkaline melts can escape upwards from a convecting mantle source.

Trindade mantle plume track

Two points lead towards the hypothesis that the source of the Serra do Mar province mafic magmas was a mantle plume:

(1) We have inferred above that the bulk of the melts originated within the OIB-source convecting mantle (McKenzie & O'Nions, 1995), beneath the base of the South American lithospheric plate.

(2) Our deduction above (Fig. 14), that the OIB-like magmas originated within the spinel → garnet transition zone, gives an estimate of ~70 km for the top of the Late Cretaceous and Palaeocene convecting mantle, beneath the lithosphere in the Serra do Mar region (Kinzler & Grove, 1992; Ionov *et al.*, 1993). This compares with the present-day thickness of 200–250 km for the São Francisco craton, to the north (Fig. 2), determined by teleseismic tomography (Grand, 1994; VanDecar *et al.*, 1995). A lithospheric thickness of ~70 km corresponds approximately to that beneath Hawaii at present (Watson & McKenzie, 1991). This is sufficient to prevent anhydrous decompression melting of convecting mantle with a potential temperature (T_p) of ~1300°C; appropriate to generating basaltic oceanic crust of 'normal' thickness (~7 km; White & McKenzie, 1995) at spreading centres. The volatile content of the Serra do Mar mafic magmas could complicate refinement of these estimates, as noted above, but the effect might not be very large in the case of basanites (Hirose & Kawamoto, 1995).

Using Hawaii as a tectonomagmatic reference point, it is apparent that the Serra do Mar region did not pass directly over a 'full power' mantle plume (thermally speaking), with T_p ~1550°C (Watson & McKenzie, 1991);

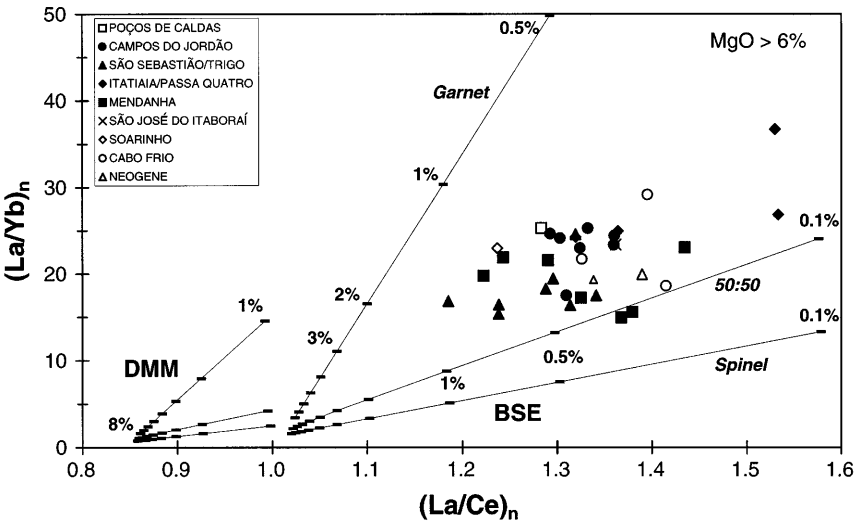

Fig. 14. Chondrite-normalized La/Yb vs La/Ce in Serra do Mar province mafic igneous rock-types. The two arrays of radiating lines refer to theoretical anhydrous lherzolite mantle partial melts, calculated according to the model of Kostopoulos & James (1992). (See text for details.)

the igneous centres of Fig. 2 are clearly not the wrecks of giant tholeiite-dominated shield volcanoes and the area lacks a Late Cretaceous flood-basalt province. Instead, the migrating magmatism is relatively small in volume and its mafic products are mostly basanites with compositions that strongly resemble those of the small-volume, post-erosion mafic alkalic volcanism of the Hawaiian islands (Fig. 11). Wyllie (1988), Watson & McKenzie (1991) and others have proposed that the Hawaiian late-stage alkalic magmas originated—at least in part—from the cooler periphery, rather than the hotter core, of the underlying mantle plume. At the times that they were erupted, the centre of the Hawaiian plume head was fuelling younger tholeiitic shield volcanoes, 200–300 km to the southeast.

The many numerical models of steady-state mantle plumes ('tails'; not their initial starting-heads) published during the last decade or so (e.g. Courtney & White, 1986; Watson & McKenzie, 1991; Ceuleneer *et al.*, 1993) all calculate sub-lithospheric plume heads with radii in the general range of ~600 km. Heat loss from a mantle plume can occur in three ways: advection via escaping melt; conduction to both the overlying lithosphere and underlying ambient-temperature convecting mantle; marginal mixing between the latter and the plume-head mantle (e.g. Sleep, 1996). Numerical models mostly agree that advective heat loss by decompression melting is largely confined to the vicinity of the core of the plume head, if a constant-thickness lithosphere is assumed (e.g. Watson & McKenzie, 1991; Ceuleneer *et al.*, 1993; Farnetani & Richards, 1995). Towards the plume-head periphery, the decrease in T_p is usually modelled as gradual and approximately linear (presumably an asymptotic curve). Viewed from this theoretical background, the convecting-mantle source of the bulk of the Serra do Mar mafic magmatism could have been: (1) the periphery of the head of a major mantle plume which lay on a track that passed several hundred kilometres away during the ~80–55 Ma interval; (2) a comparatively minor local upper-mantle thermal disturbance.

The initiation of Serra do Mar magmatism migrated ESE for 500 km across the province, from Poços de Caldas to Cabo Frio, between 80 Ma (or slightly earlier) and ~55 Ma. If this represents magmatism from a source fixed within the global hotspot framework, penetrating a drifting plate, the apparent plate migration velocity was 2·0 cm/yr, a figure little more than half that of the South American plate (O'Connor & Duncan, 1990; Müller *et al.*, 1993). Between our first published reports of these results (Thompson *et al.*, 1997*a*, 1997*b*) and the completion of this paper, R. W. Carlson (personal communication, 1997) has informed us that he has also detected this migrating magmatism, based on Rb/Sr isochron studies of the syenite complexes. Can magmatism migrating at far less than the drift rate of the South Atlantic plate be plausibly related to a mantle plume? Figure 15 shows how the Trindade mantle plume might fit this tectonomagmatic scenario. Nevertheless, although it has appeared in most discussions of the topic on a global scale, and also in many others concentrating on South Atlantic tectonomagmatic relationships (e.g. Crough *et al.*, 1980; O'Connor & Duncan, 1990), we must first summarize the evidence that a mantle plume currently centred approximately beneath Trindade and Martin Vaz actually exists.

VanDecar *et al.* (1995) have suggested that there is no such mantle plume and that the magmatism forming

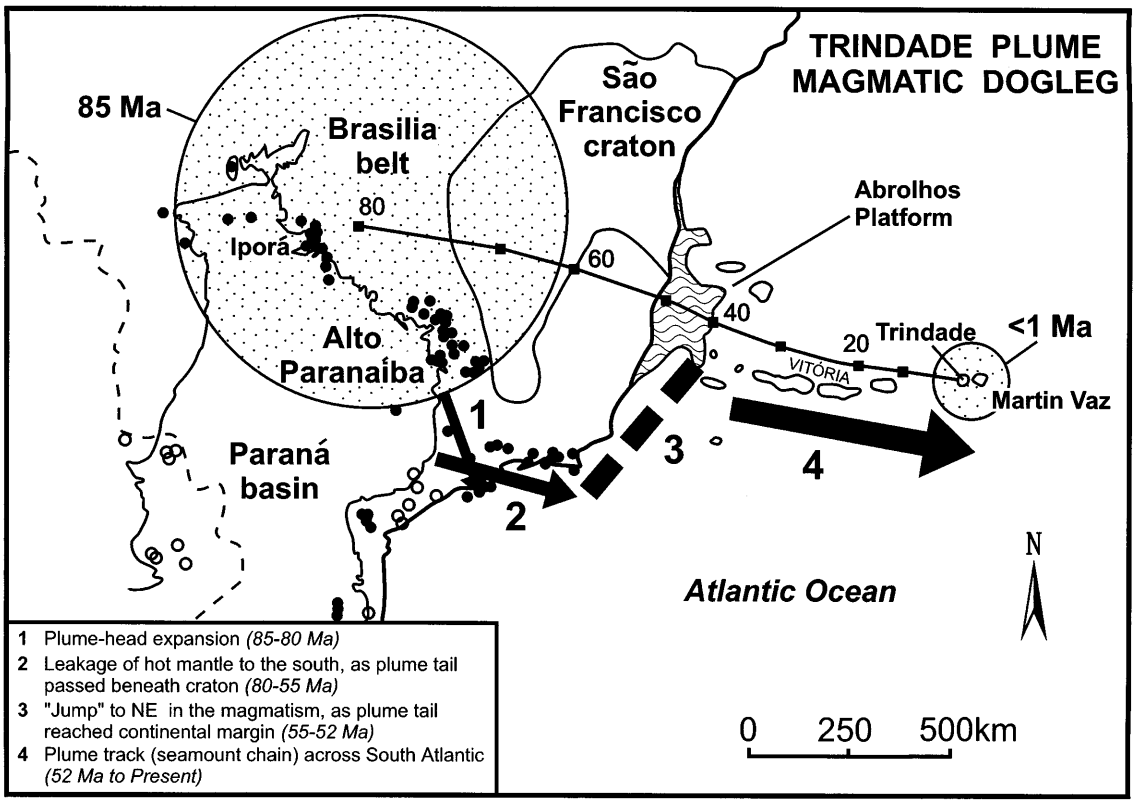

Fig. 15. Sketch map of SE Brazil summarizing the sequence of magmatic events since ~90 Ma and our interpretation of them. (See Fig. 1 for the regional context of the on-land geology.) Open and filled circles are Early and Late Cretaceous–Palaeogene complexes, respectively. The large patterned circle marks the area postulated to have been underlain at ~85 Ma by the hot head of the Trindade starting-mantle plume (Gibson *et al.*, 1995, 1997*c*). The tail of this plume (shown schematically by a small patterned circle) is now thought to underlie the islands of Trindade and Martin Vaz. Experimental and numerical studies of mantle plumes (e.g. Davis, 1995; Farnetani & Richards, 1995) all show that the transition from large-volume starting-plume head to lower-flux plume tail occurs soon (a few million years) after the initial sub-lithospheric starting-plume impact. Seamounts of the Vitória chain, linking Trindade and the Abrolhos Platform, are outlined. The curved line, with labels beside it at 20 my intervals, is the calculated track of the Trindade plume, using the plate-tectonic framework of Müller *et al.* (1993). (See text for a full discussion of the numbered arrows and dashed line.) Whereas the term 'dogleg' is clear to English speakers, it does not translate successfully into Brazilian Portuguese, where 'geo-lombada' would be more appropriate.

Trindade, Martin Vaz and the Vitória seamount chain, between Trindade and the Brazilian mainland (Fig. 15), is only the result of a 'leaky transform fault'. This suggestion may be evaluated by considering the end-member case of leaky transform faults, which is a spreading centre. Over convecting mantle with the global ambient potential temperature of ~1300°C, a spreading centre generates oceanic crust of normal (~7 km) thickness, not a seamount chain. Trindade and Martin Vaz are built on oceanic crust >70 Ma in age; oceanic lithosphere of this age is ~120 km thick, with an ~90 km thick mechanical boundary layer (Parsons & McKenzie, 1978). Trindade and Martin Vaz rise from a broad topographic swell beneath water 5 km deep. Trindade reaches ~600 m above sea level, and its total height is thus ~5·5 km. Trindade is therefore a volcano that is similar in height to those of the Hawaiian islands, although steeper sided and therefore less voluminous, and it is built on lithosphere which is probably somewhat thicker than and drifting at a similar velocity to that beneath Hawaii (Müller *et al.*, 1993). We can see no realistic alternative to the view that a mantle plume currently underlies Trindade–Martin Vaz. Likewise, the major Vitória chain seamounts all rise up to 4·5 km above seafloor. The short-wavelength positive geoid anomalies associated with Trindade and the Vitória seamounts have been documented by Fleitout *et al.* (1989) and Ussami & Molina (1997).

Figure 15 shows the calculated track of a mantle plume, currently beneath Trindade (most recent magmatism at ~20 ka; Cordani, 1970), back to 80 Ma. The input was a global set of parameters for absolute plate motions, back to chron 34 (84 Ma), derived by Müller *et al.* (1993) from a best fit to 'radiometrically-dated hotspot tracks on the Australian, Indian, African, North and South American plates, relative to present-day hotspots assumed fixed in the mantle'. The calculated track bisects the

Abrolhos Platform—a constructional magmatic feature resembling a small flood basalt province (Fodor *et al.*, 1989)—and is predicted to have passed beneath its site at the time that the magmatism occurred (42–52 Ma; Cordani, 1970). We do not know whether there is any significance in the small divergence between the post-40 Ma calculated plume track and the trend of the Vitória seamount chain (Fig. 15). If the divergence is real, a possible explanation is that the plume-head magmatism escaped upwards via the line of weakness presented by the Martin Vaz fracture zone, rather than penetrating the lithosphere directly above. Nevertheless, there is continuing controversy as to whether or not plumes drift, relative to each other, and hence whether plume tracks can indeed be reconstructed in the manner of Fig. 15 (Harada, 1997; Raymond *et al.*, 1997). The large circle marked in Fig. 15 shows the postulated impact site of the Trindade starting-mantle-plume head at ~85 Ma, as deduced by Gibson *et al.* (1995, 1997*c*). In Fig. 15 we have specified three stages in the post-impact subcontinental migration of the Trindade plume and associated magmatism:

(1) *Expansion of the starting-plume head (85–80 Ma).* The conventional circular starting-plume impact site drawn in Fig. 15 gives no obvious explanation for magmatism beginning at Poços de Caldas at ~84 Ma (Shea, 1992) and at the offshore island group, São Sebastião–Ilhabela, Trigo, Vitória and Buzios, at ~80 Ma (Figs 2 and 6). A possible explanation might be that the starting-plume head expanded rapidly until it decompressed, began to melt and 'leaked' magma beneath the thinner lithosphere of the stretched continental passive margin (Hill, 1991; Thompson & Gibson, 1991; Sleep, 1996, 1997). Recent studies of fission-track data support this concept. Hegarty *et al.* (1996) used apatite fission-track analyses of samples from within and around the southern part of the Paraná basin (Fig. 1) to detect an episode of substantial uplift and subsequent kilometre-scale erosion (causing crustal cooling) between 90 and 80 Ma. Harman *et al.* (1997) have reported comparable data from sites on the São Francisco craton, and Gallagher & Brown (1997) have shown how the coastal margin of SE Brazil has undergone substantial uplift and erosion in the 90–60 Ma interval, long after the initiation of the South Atlantic at ~130 Ma. Hegarty *et al.* (1996) noted that their data could be explained well by the impact of a late Cretaceous starting-mantle plume beneath the region.

A difficulty with such an interpretation is the large distance (~1200 km) between the parts of southern Brazil and eastern Paraguay that show evidence for this late Cretaceous uplift and the centre of the starting-plume impact site marked in Fig. 15. Figure 1 shows a possible explanation. The northern side of the proposed Trindade starting-plume impact site is largely ringed by the Amazonas and São Francisco cratons. Perhaps the deep lithospheric keels of these cratons impeded plume-head expansion northwards, thus accentuating it southwards. The Trindade starting-plume head may also have been unusually hot and buoyant, during its post-impact expansion, because at first it underlay lithosphere too thick to permit significant decompression melting (Gibson *et al.*, 1995, 1997*c*) and consequential rapid escape of heat (Sleep, 1996, 1997). We note that the plume-head expansion model, proposed here, also gives a plausible explanation for the late Cretaceous igneous centres within the Ponta Grossa igneous province (Fig. 1) and the local rifting-related alkaline magmatism around Lages at 80–75 Ma (Sonoki & Garda, 1988; Gibson *et al.*, in preparation).

(2) *Leakage of hot plume-tail mantle to the south, as the plume passed beneath a craton (80–55 Ma).* Magmatism is spatially associated with the calculated Trindade plume track, both before 80 Ma and after 52 Ma (Fig. 15). Between these times the calculated track lay beneath the São Francisco craton, whereas contemporaneous alkaline magmatism migrated ESE across the Serra do Mar region (Figs 2 and 6), ~500 km to the south. We propose that this magmatism was fed by a southward flow of hot plume-tail mantle from beneath the São Francisco craton. The migrating row of complexes is oblique to basement structural trends (Fig. 2). We suggest that, in general, the magmas were generated (and erupted) at the first points south of the craton where the slowly cooling flow of plume-tail mantle arrived beneath lithosphere, within the rapidly thinning zone adjacent to the continental margin, where significant decompression melting could occur (Thompson & Gibson, 1991; Sleep, 1996, 1997). This leakage process broke the direct connection between the fixed-site mantle plume and the magmas eventually produced by its decompression melting. As a result, the Serra do Mar magmatism migrated ESE at ~2·0 cm/yr (Fig. 6), about half the rate of 3·6 cm/yr calculated for the theoretical plume track (Fig. 15). This implies that great care should be taken before deducing that a belt of migrating magmatism on a continent necessarily measures its drift rate.

(3) *'Jump' to NE in the magmatism, as the plume tail reached the continental margin (55–52 Ma).* The Serra do Mar province migrating magmatism ceased abruptly in the Cabo Frio area at 55 Ma (Figs 2 and 6); there are no appropriate seamounts offshore along the continuation of this trend. Instead, the Abrolhos Platform large-scale magmatism began at essentially the same time, ~400 km to the northeast. We suggest that, as the Trindade plume tail reached the thinner lithosphere of the continental margin, to the east of the São Francisco craton, it was able to decompress sufficiently to initiate substantial melting and thus to cut the southward flow of hot mantle towards the Serra do Mar igneous province. It should be noted that our discussion of how the hot mantle of the Trindade plume may have behaved beneath the

lithosphere of SE Brazil between 85 and 50 Ma is written in similar terms to a description of water drainage (hot mantle) on an irregular surface (base of lithosphere), except that the system is upside down. In this approach we follow Sleep (1996, 1997), who has quantified some aspects of such a tectonomagmatic model.

SUMMARY

(1) The predominantly syenitic complexes of the ~80–55 Ma Serra do Mar igneous province, SE Brazil, are accompanied by minor amounts of mafic magmatism, emplaced as dykes (mostly), sills and lavas.

(2) In a few instances the hypabyssal sheets cut the syenites. Mostly they occur in Brasiliano (Pan-African; ~750–450 Ma) Ribera belt basement, within ~10 km of each plutonic complex.

(3) Most of the Serra do Mar mafic rocks are basanites; some are basalts or melanephelinites (Fig. 7). A few samples are picritic (Table 2).

(4) Although most samples have similar K/Na ratios to those of lavas reported from Trindade island, South Atlantic (Fig. 8), more potassic mafic rock-types also occur sporadically throughout the province: leucitite blocks (variably analcitized) in agglomerate at Poços de Caldas; lava with chloritized phlogopite phenocrysts at São José do Itaboraí; a sparsely phlogopite-phyric dyke at Campos do Jordão; minette dykes at Itatiaia, Tinguá, Soarinho and Cabo Frio.

(5) The major- and trace-element and Sr–Nd isotopic compositions of some of the Serra do Mar basanite dykes overlap those of Trindade lavas. Other Serra do Mar mafic samples show a geochemical range towards the compositional field of SE Brazil late Cretaceous potassic mafic–ultramafic magmas that are considered to originate from lithospheric mantle sources (Gibson *et al.*, 1996).

(6) Two picrites show geochemical evidence of contamination with upper crust; they probably flowed turbulently during emplacement (ATA).

(7) Forward modelling, using REE ratios, suggests that most Serra do Mar mafic magmas were generated by ~0·1–1·0% partial melting of an OIB-source-like lherzolite mantle beneath an ~70 km lithosphere.

(8) Trindade and Martin Vaz are volcanoes rising 5–5·5 km above the sea-floor, which have been constructed during the last ~3 my on >70 Ma oceanic crust (i.e. lithosphere ~120 km thick, with MBL ~90 km; similar to or thicker than beneath Hawaii). Such characteristics support the view that they are products of a mantle plume that also generated the Vitória seamount chain and Abrolhos Platform. Short-wavelength positive geoid anomalies characterize Trindade and the Vitória seamounts (Fleitout *et al.*, 1989; Ussami & Molina, 1997).

(9) Extensive synchronous magmatism at ~85 Ma in central and SE Brazil originated from both lithospheric (mostly) and OIB-source subjacent convecting mantle (Gibson *et al.*, 1995, 1997*c*). The reconstructed track of the Trindade plume places it close to Brasília at 85–80 Ma. Both the widespread ~85 Ma magmatism, and extensive uplift and erosion throughout southern Brazil and Paraguay (apatite fission-track data of Hegarty *et al.*, 1996; Gallagher & Brown, 1997; Harman *et al.*, 1997), are consistent with the hypothesis that the Trindade starting-mantle plume impacted at ~85 Ma and its buoyant head spread 1000 km or more southwards, beneath thick lithosphere.

(10) Between ~85 and 52 Ma the predicted track of the Trindade plume tail passed amagmatically beneath the São Francisco craton at ~3·6 cm/yr, as the South American plate drifted westward. Physical evidence that this actually happened is preserved as a linear positive geoid anomaly, extending beneath the southern São Francisco craton, between Alto Paranaíba and the Vitória seamount chain (Fig. 15). Ussami & Molina (1997) attributed this to a thermal disturbance at the base of the lithosphere, as might occur if it drifted over the tail of a mantle plume.

(11) In the same time interval, a row of igneous centres formed progressively along an ESE trend across the relatively thin lithosphere of the Serra do Mar region, ~500 km south of the predicted Trindade plume track. The initiation of this magmatism migrated at ~2·0 cm/yr.

(12) We propose that, between ~80 and 55 Ma, hot upwelling Trindade plume-tail mantle was deflected by the deep lithospheric root of the São Francisco craton and flowed south until it could decompress and partially melt beneath thinner lithosphere under an adjacent former mobile belt (Hill, 1991; Thompson & Gibson, 1991; Sleep, 1996, 1997).

ACKNOWLEDGEMENTS

This work was funded by NERC (UK) Research Grant GR3/8084, NSERC (Canada), CNPq (Brazil) and the British Council, together with additional financial and logistical input from the Universities of Brasília, Cambridge, Durham and Newcastle upon Tyne. We thank Yvonne Brown, Ron Hardy, Chris Ottley, Graham Pearson and Rob Ridley for their technical assistance with elemental and isotopic analyses, and Roger Searle for calculating the theoretical Trindade plume track. J. M. V. Coutinho, J. G. Valença, and H. H. G. L. and M. N. C. Ulbrich were generous with their time, advice and practical assistance, in connection with our fieldwork. Countless landowners and quarry managers allowed us access to outcrops; the manager of the Sentíssimo quarry

earned our heartfelt thanks for whisking us to safety when the gunfire came too close for comfort. Vicky Hards made a crucial contribution by joining a depleted fieldwork team at zero notice, allowing the sampling of the offshore islands. Comments by Mike Coffin, Tony Ewart, Vicky Hards, Teresa Junqueira-Brod, Graham Pearson and Marge Wilson substantially improved the text.

REFERENCES

Amorim, M. S., Sichel, S. E. & Meighan, I. (1995). Estudo preliminar dos elementos terras raras dos maciços alcalinos de Tanguá, Rio Bonito, Morro de São João e Itaúna, RJ. *V Congresso Brasileiro de Geoquímica*, Niterói/RJ. (No page numbers. This publication is only available as a CD-ROM from Sociedade Brasileira de Geoquímica, Rio de Janeiro.)

Araújo, A. L. N., Sichel, S. E. & Valença, J.G. (1995). Geoquímica das rochas alcalinas de Arraial do Cabo (RJ): Ilha do Cabo Frio e áreas continentais adjacentes. *V Congresso Brasileiro de Geoquímica*, Niterói/RJ. (No page numbers. This publication is only available as a CD-ROM from Sociedade Brasileira de Geoquímica, Rio de Janeiro.)

Bellieni, G., Montes-Lauar, C. R., De Min, A., Piccirillo, E. M., Cavazzini, G., Melfi, A. J. & Pacca, I. G. (1990). Early- and Late-Cretaceous magmatism from São Sebastião island (SE Brazil): geochemistry and petrology. *Geochimica Brasiliensis* **4,** 59–83.

Brotzu, P., Beccaluva, L., Conte, A., Fonseca, M., Gabarino, C., Gomes, C. B., Leong, R., Macciotta, G., Mansur, R. L., Melluso, L., Morbidelli, L., Ruberti, E., Sigolo, J. B., Traversa, G. & Valença, J. G. (1989). Petrological and geochemical studies of alkaline rocks from continental Brazil, 8: The syenitic intrusion of Morro Redondo, RJ. *Geochimica Brasiliensis* **3,** 63–80.

Brotzu, P., Barbieri, M., Beccaluva, L., Gabarino, C., Gomes, C. B., Macciotta, G., Melluso, L., Morbidelli, L., Ruberti, E., Sigolo, J. B. & Traversa, G. (1992). Petrology and geochemistry of the Passa Quatro alkaline complex, southeastern Brazil. *Journal of South American Earth Sciences* **6,** 237–252.

Brotzu, P., Gomes, C. B., Melluso, L., Morbidelli, L., Morra, V. & Ruberti, E. (1995). Petrologia do maciço alcalino de Itatiaia, RJ-MG-SP. *V Congresso Brasileiro de Geoquímica*, Niterói/RJ. (No page numbers. This publication is only available as a CD-ROM from Sociedade Brasileira de Geoquímica, Rio de Janeiro.)

Brotzu, P., Gomes, C. B., Melluso, L., Morbidelli, L., Morra, V. & Ruberti, E. (1997). Petrogenesis of coexisting SiO_2-undersaturated to SiO_2-saturated felsic igneous rocks: the alkaline complex of Itatiaia, southeastern Brazil. *Lithos* **40,** 133–156.

Carlson, R. W., Esperança, S. & Svisero, D. P. (1996). Chemical and Os isotopic study of Cretaceous potassic rocks from southern Brazil. *Contributions to Mineralogy and Petrology* **125,** 393–405.

Ceuleneer, G., Monnereau, M., Rabinowicz, M. & Rosemberg, C. (1993). Thermal and petrological consequences of melt migration within mantle plumes. *Philosophical Transactions of the Royal Society of London, Series A* **342,** 53–64.

Chang, H. K., Kowsmann, R. O., Figueiredo, A. M. F. & Bender, A. A. (1992). Tectonics and stratigraphy of the East Brazil Rift system: an overview. *Tectonophysics* **213,** 97–138.

Cima, A. R. B. (1995). Geochronology and petrology of the Cretaceous mafic potassic rocks from Paraguay and Brazil. M.Sc. Thesis, University of Newcastle upon Tyne, 104 pp.

Comin-Chiaramonti, P., Cundari, A., Piccirillo, E. M., Gomes, C. B., Castorina, F., Censi, P., De Min, A., Marzoli, A., Speziale, S. & Velázquez, V. F. (1997). Potassic and sodic igneous rocks from eastern Paraguay: their origin from the lithospheric mantle and genetic relationships with the associated Paraná flood tholeiites. *Journal of Petrology* **38,** 495–528.

Cordani, U. G. (1970). Idade do vulcanismo no Oceano Atlântico. *Boletim do Instituto Astronômico e Geofísico, Universidade de São Paulo* **1,** 9–75.

Cordery, M. J., Davis, G. F. & Campbell, I. H. (1997). Genesis of flood basalts from eclogite-bearing mantle plumes. *Journal of Geophysical Research* **102,** 20179–20197.

Courtney, R. C. & White, R. S. (1986). Anomalous heat flow and geoid across the Cape Verde Rise: evidence of dynamic support from a thermal plume in the mantle. *Geophysical Journal of the Royal Astronomical Society* **87,** 815–867.

Crough, S. T., Morgan, W. J. & Hargreaves, R. B. (1980). Kimberlites: their relation to mantle hot spots. *Earth and Planetary Science Letters* **50,** 260–274.

Davis, G. F. (1995). Penetration of plates and plumes through the mantle transition zone. *Earth and Planetary Science Letters* **133,** 507–516.

Deer, W. A., Howie, R. A. & Zussman, J. (1965). *Rock Forming Minerals 3, Sheet Silicates*. London: Longmans, 270 pp.

Farnetani, D. G. & Richards, M. A. (1995). Thermal entrainment and melting in mantle plumes. *Earth and Planetary Science Letters* **136,** 251–267.

Fitton, J. G., James, D. & Leeman, W.P. (1991). Basic magmatism associated with Late Cenozoic extension in the western United States: compositional variations in space and time. *Journal of Geophysical Research* **96,** 13693–13711.

Fleitout, L., Dalloubeix, C. & Moriceau, C. (1989). Small-wavelength geoid and topography anomalies in the South Atlantic Ocean: a clue to new hot-spot tracks and lithospheric deformation. *Geophysical Research Letters* **16,** 637–640.

Fodor, R. V., Mukasa, S. B., Gomes, C. B. & Cordani, U. G. (1989). Ti-rich Eocene basaltic rocks, Abrolhos Platform, offshore Brazil, 18°S: petrology with respect to South Atlantic magmatism. *Journal of Petrology* **30,** 763–786.

Fonseca, A. C., Cordani, U. G., Bigazzi, G. & Kawaaskita, K. (1995). Evolução geocronológica da região de Cabo Frio, Rio de Janeiro, e seu significado na correlação Brasil–África. *V Congresso Brasileiro de Geoquímica*, Niterói/RJ. (No page numbers. This publication is only available as a CD-ROM from Sociedade Brasileira de Geoquímica, Rio de Janeiro.)

Gallagher, K. & Brown, R. (1997). The onshore record of passive margin evolution. *Journal of the Geological Society, London* **154,** 451–457.

Gallagher, K., Hawkesworth, C. J. & Mantovani, M. S. M. (1994). The denudation history of the onshore continental margin of SE Brazil inferred from apatite fission track data. *Journal of Geophysical Research* **99,** 18117–18145.

Garda, G. M., Schorscher, J. H. D., Esperança, S. & Carlson, R. W. (1995). The petrology and geochemistry of coastal dikes from São Paulo State, Brazil: implications for variable lithospheric contributions to alkaline magmas from the western margin of the South Atlantic. *Anais da Academia Brasileira de Ciências* **67,** 191–216.

Gibson, S. A., Thompson, R. N., Leonardos, O. H., Turner, S. P., Mitchell, J. G. & Dickin, A. P. (1994). The Serra do Bueno potassic diatreme: a possible hypabyssal equivalent of the ultramafic alkaline volcanics in the Late Cretaceous Alto Paranaíba Igneous Province, SE Brazil. *Mineralogical Magazine* **58,** 357–372.

Gibson, S. A., Thompson, R. N., Leonardos, O. H., Dickin, A. P. & Mitchell, J. G. (1995). The Late Cretaceous impact of the Trindade mantle plume: evidence from large-volume, mafic, potassic magmatism in SE Brazil. *Journal of Petrology* **36,** 189–229.

Gibson, S. A., Thompson, R. N., Dickin, A. P. & Leonardos, O. H. (1996). High-Ti and low-Ti mafic potassic magmas: key to plume–lithosphere interactions and continental flood-basalt genesis. *Earth and Planetary Science Letters* **141,** 325–341.

Gibson, S. A., Thompson, R. N., Dickin, A. P. & Mitchell, J. G. (1997*a*). Temporal variation in magma sources related to the impact of the Tristan mantle plume. *International Symposium on Plumes, Plates and Mineralisation (PPM'97)*. Pretoria, South Africa, 37–38.

Gibson, S. A., Thompson, R. N., Dickin, A. P., Mitchell, J. G. & Milner, S. C. (1997*b*). Temporal variation in magma sources related to the impact of the Tristan mantle plume. *Journal of Conference Abstracts* **2,** 32.

Gibson, S. A., Thompson, R. N., Weska, R., Dickin, A. P. & Leonardos, O. H. (1997*c*). Late Cretaceous rift-related upwelling and melting of the Trindade starting mantle plume head beneath western Brazil. *Contributions to Mineralogy and Petrology* **126,** 303–314.

Grand, S. P. (1994). Mantle shear structure beneath the Americas and surrounding oceans. *Journal of Geophysical Research* **99,** 11591–11621.

Gresse, P. G., Chemale, F., da Silva, L. C., Walraven, F. & Hartmann, L. A. (1996). Late- to post-orogenic basins of the Pan-African–Brasiliano collision orogen in southern Africa and southern Brazil. *Basin Research* **8,** 157–171.

Halliday, A. N., Davies, G. R., Lee, D.-C., Tommasini, S., Paslick, C. R., Fitton, J. G. & James, D. E. (1992). Lead isotopic evidence for young trace element enrichment in the oceanic upper mantle. *Nature* **359,** 623–627.

Hamilton, M. A., Pearson, D. G., Thompson, R. N., Kelley, S. P. & Emeleus, C. H. (1998). Rapid eruption of Skye lavas inferred from precise U–Pb and Ar–Ar dating of the Rum and Cuillin plutonic complexes. *Nature* **392,** in press.

Harada, Y. (1997). New accurate models of the plate motions relative to the hotspots and the cause of the discrepancy in the global plate-motion circuit. *Eos Transactions, American Geophysical Union* **78,** 721.

Harman, R., Gallagher, K. & Brown, R. (1997). Long term denudation and tectonics in the cratons of northern Brazil. *Terra Nova* **9,** 68.

Hartnady, C. J. H. & le Roex, A. P. (1985). Ocean hot spot tracks and the Cenozoic absolute motion of the African, Antarctic and South American plates. *Earth and Planetary Science Letters* **75,** 245–257.

Hegarty, K. A., Duddy, I. R. & Green, P. F. (1996). The thermal history in and around the Paraná Basin using apatite fission track analysis—implications for hydrocarbon occurrences and basin formation. In: Comin-Chiaramonti, P. & Gomes, C. B. (eds) *Alkaline Magmatism in Central–Eastern Paraguay: Relationships with Coeval Magmatism in Brazil*. São Paulo: Edusp–Fapesp, pp. 67–83.

Herz, N. (1977). Timing of spreading in the South Atlantic: information from Brazilian alkalic rocks. *Geological Society of America Bulletin* **88,** 101–112.

Hill, R. I. (1991). Starting plumes and continental break-up. *Earth and Planetary Science Letters* **104,** 398–416.

Hirose, K. & Kawamoto, T. (1995). Hydrous partial melting of lherzolite at 1 GPa: the effect of H_2O on the genesis of basaltic magmas. *Earth and Planetary Science Letters* **133,** 463–473.

Hofmann, A. W. (1997). Mantle geochemistry: the message from oceanic volcanism. *Nature* **385,** 219–229.

Huppert, H. E. & Sparks, R. S. J. (1985). Cooling and contamination of mafic and ultramafic magmas during ascent through continental crust. *Earth and Planetary Science Letters* **74,** 371–386.

Ionov, D. A., Aschepkov, I. V., Stosch, H. G., Witt-Eickschen, G. & Seck, H. A. (1993). Garnet peridotite xenoliths from the Vitim volcanic field, Baikal region: the nature of the garnet–spinel peridotite transition zone in the continental mantle. *Journal of Petrology* **34,** 1141–1175.

Kerr, A. C., Kempton, P. D. & Thompson, R. N. (1995). Crustal assimilation during turbulent magma ascent (ATA); new isotopic evidence from the Mull Tertiary lava succession, N. W. Scotland. *Contributions to Mineralogy and Petrology* **119,** 142–154.

Kille, I. C., Thompson, R. N., Morrison, M. A. & Thompson, R. F. (1986). Field evidence for turbulence during flow of basalt magma through conduits from southwest Mull. *Geological Magazine* **123,** 693–697.

King, S. D. & Anderson, D. L. (1995). An alternative mechanism of flood basalt formation. *Earth and Planetary Science Letters* **136,** 269–279.

Kinzler, R. J. & Grove, T. L. (1992). Primary magmas of mid-ocean-ridge basalts. 1. Experiments and methods. *Journal of Geophysical Research* **97,** 6885–6906.

Klein, V. C. & Valença, J. G. (1984). Estruturas almofadadas em derrame ankaramítico na bacia de São José do Itaboraí, Rio de Janeiro. *Anais do XXXIII Congresso Brasileiro de Geologia*, Rio de Janeiro, pp. 4335–4345.

Klein, V. C., Valença, J. G. & Vieira, A. C. (1984). Ignimbritos do vulcão de Nova Iguaçú e da 'Chaminé do Lamego', Rio de Janeiro. *Anais do XXXIII Congresso Brasileiro de Geologia*, Rio de Janeiro, 4346–4354.

Kostopoulos, D. K. & James, S. D. (1992). Parameterisation of the melting regime of the shallow upper mantle and the effects of variable lithospheric stretching on mantle modal stratification and trace-element concentrations in magmas. *Journal of Petrology* **33,** 665–691.

Le Maitre, R. W. (1989). *A Classification of Igneous Rocks and Glossary of Terms*. Oxford: Blackwell, 193 pp.

Lima, P. R. A. S. (1976). Geologia dos maciços alcalinos do estado do Rio de Janeiro. *Semana de Estudos Geológicos*, Itaguaí, pp. 205–259.

Machado, N., Valladares, C., Heilbron, M. & Valeriano, C. (1996). U–Pb geochronology of the central Ribeira belt (Brazil) and implications for the evolution of the Brazilian Orogeny. *Precambrian Research* **79,** 347–361.

McKenzie, D. (1984). A possible mechanism for epeirogenic uplift. *Nature* **307,** 616–618.

McKenzie, D. (1989). Some remarks on the movement of small melt fractions in the mantle. *Earth and Planetary Science Letters* **95,** 53–72.

McKenzie, D. & O'Nions, R. K. (1991). Partial melt distributions from inversion of rare-earth element concentrations. *Journal of Petrology* **32,** 1021–1091.

McKenzie, D. & O'Nions, R. K. (1995). The source regions of ocean-island basalts. *Journal of Petrology* **36,** 133–160.

Menzies, M. A. (1989). Cratonic, circumcratonic and oceanic mantle domains beneath the western United States. *Journal of Geophysical Research* **94,** 7899–7915.

Milner, S. C. & le Roex, A. P. (1996). Isotope characteristics of the Okenyenya igneous complex, northwestern Namibia: constraints on the composition of the early Tristan plume and the origin of the EM 1 mantle component. *Earth and Planetary Science Letters* **141,** 277–291.

Milner, S. C., le Roex, A. P. & O'Connor, J. M. (1995). Age of the Mesozoic igneous rocks of northwestern Namibia, and their relationship to continental breakup. *Journal of the Geological Society, London* **152,** 97–104.

Mitchell, R. H. & Bergman, S. C. (1991). *Petrology of Lamproites*. New York: Plenum Press, 447 pp.

Mohriak, W. U., Rabelo, J. H. L., Matos, R. D. & Barros, M. C. (1995). Deep seismic reflection profiling of sedimentary basins off-shore Brazil: geological objectives and preliminary results in the Sergipe Basin. *Journal of Geodynamics* **20,** 515–539.

Molyneux, S. J. (1997). Processes of granite emplacement: NW Ireland and SE Brazil. Ph.D. Thesis, University of Durham.

Montes-Lauar, C. R., Pacca, I. G., Melfi, A. J. & Kawashita, K. (1995). Late Cretaceous alkaline complexes, southeastern Brazil: paleomagnetism and geochronology. *Earth and Planetary Science Letters* **134,** 425–440.

Moorbath, S. & Thompson, R.N. (1980). Strontium isotope geochemistry and petrogenesis of the Early Tertiary lava pile of the Isle of Skye, Scotland, and other basic rocks of the British Tertiary Province: an example of magma–crust interaction. *Journal of Petrology* **21,** 295–321.

Morbidelli, L., Gomes, C. B., Beccaluva, L., Brotzu, P., Conte, A. M., Ruberti, E. & Traversa, G. (1995). Mineralogical, petrological and geochemical aspects of alkaline and alkaline–carbonatite associations from Brazil. *Earth-Science Reviews* **30,** 135–168.

Morgan, W. J. (1983). Hot spot tracks and the early rifting of the Atlantic. *Tectonophysics* **94,** 123–139.

Müller, R. D., Royer, J.-Y. & Lawver, L. A. (1993). Revised plate motions relative to hotspots from combined Atlantic and Indian Ocean hotspot tracks. *Geology* **21,** 275–278.

O'Connor, J. M. & Duncan, R. A. (1990). Evolution of the Walvis Ridge–Rio Grande Rise hot spot system: implications for African and South American plate motions over plumes. *Journal of Geophysical Research* **95,** 17475–17502.

Parsons, B. & McKenzie, D. P. (1978). Mantle convection and the thermal structure of the plates. *Journal of Geophysical Research* **83,** 4485–4496.

Raymond, C. A., Stock, J. M. & Cande, S. C. (1997). Pacific hotspot relative motion. *Eos Transactions, American Geophysical Union* **78,** 183.

Regelous, M. (1993). Geochemistry of dolerites from the Paraná flood basalt province, southern Brazil. Ph.D. Thesis, Open University, Milton Keynes, UK, 256 pp.

Renne, P. R., Mertz, D. F., Ernesto, M., Marques, L., Teixeira, W., Ens, H. H. & Richards, M. A. (1993). Geochronologic constraints on magmatic and tectonic evolution of the Paraná province. *Eos Transactions, American Geophysical Union* **74,** 553.

Renne, P. R., Glen, J. M., Milner, S. C. & Duncan, A. R. (1996). Age of Etendeka flood volcanism and associated intrusions in southwestern Africa. *Geology* **24,** 659–662.

Richards, M. A., Bunge, H.-P., Baumgardner, J. R. & Lithgow-Bertelloni, C. (1997). Geodynamic models of deep Earth structure. *Terra Nova* **9,** 39.

Schobbenhaus, C., Campos, D. A., Derze, G. R. & Asmus, H. E. (1984). *Geologia do Brasil*. Brasilia-DF: DNPM, 501 pp.

Schorscher, H. D. & Shea, M. E. (1992). The regional geology of the Poços de Caldas alkaline complex: mineralogy and geochemistry of selected nepheline syenites and phonolites. *Journal of Geochemical Exploration* **45,** 25–51.

Shaw, D. M. (1979). Trace element melting models. *Physics and Chemistry of the Earth* **11,** 577–586.

Shea, M. E. (1992). Isotopic geochemical characterization of selected nepheline syenites and phonolites from the Poços de Caldas alkaline complex, Minas Gerais, Brazil. *Journal of Geochemical Exploration* **45,** 173–214.

Sleep, N. H. (1996). Lateral flow of hot plume material ponded at sublithospheric depths. *Journal of Geophysical Research* **101,** 28065–28083.

Sleep, N. H. (1997). Lateral flow and ponding of starting plume material. *Journal of Geophysical Research* **102,** 10001–10012.

Sonoki, I. K. & Garda, G. M. (1988). Idades K–Ar de rochas alcalinas do Brasil Meridional e Paraguai Oriental: compilação e adaptação às novas constantes de decaimento. *Bolletim do IG-USP, Serie Científica* **19,** 63–85.

Steiger, R. H. & Jäger, E. (1977). Convention on the use of decay constraints in geo- and cosmochronology. *Earth and Planetary Science Letters* **86,** 359–362.

Teixeira, W., Carneiro, M. A., Noce, C. M., Machado, N., Sato, K. & Taylor, P. N. (1996). Pb, Sr and Nd isotope constraints on the Archaean evolution of gneissic–granitoid complexes in the southern São Francisco craton, Brazil. *Precambrian Research* **78,** 151–164.

Thompson, R. N. & Gibson, S. A. (1991). Subcontinental mantle plumes, hot spots and pre-existing thinspots. *Journal of the Geological Society, London* **148,** 973–977.

Thompson, R. N. & Gibson, S. A. (1994). Magmatic expression of lithospheric thinning across continental rifts. *Tectonophysics* **233,** 41–68.

Thompson, R. N., Morrison, M. A., Hendry, G. L. & Parry, S. J. (1984). An assessment of the relative roles of crust and mantle in magma genesis: an elemental approach. *Philosophical Transactions of the Royal Society of London, Series A* **310,** 549–590.

Thompson, R. N., Gibson, S. A., Mitchell, J. G., Dickin, A. P., Leonardos, O. H., Brod, J. A. & Greenwood, J. C. (1997*a*). Migrating Cretaceous–Eocene magmatism in the Serra do Mar alkaline province, SE Brazil: the dog-legged track of a devious Trindade mantle plume. *Journal of Conference Abstracts* **2,** 76.

Thompson, R. N., Gibson, S. A., Mitchell, J. G., Dickin, A. P., Leonardos, O. H., Brod, J. A. & Greenwood, J. C. (1997*b*). Late-Cretaceous alkalic magmatism and mineralisation in SE Brazil: the role of the Trindade mantle plume. *International Symposium on Plumes, Plates and Mineralisation (PPM'97)*. Pretoria: University of Pretoria, pp. 103–104.

Thompson, R. N., Velde, D., Leat, P. T., Morrison, M. A., Mitchell, J. G., Dickin, A. P. & Gibson, S. A. (1997*c*). Oligocene lamproite containing a new biotite variant, Middle Park, northwest Colorado, USA. *Mineralogical Magazine* **61,** 557–572.

Turner, S., Hawkesworth, C., Gallagher, K., Stewart, K., Peate, D. & Mantovani, M. (1996). Mantle plumes, flood basalts and thermal models for melt generation beneath continents: assessment of a conductive heating model and application to the Paraná. *Journal of Geophysical Research* **101,** 11503–11518.

Ulbrich, H. H. G. J. & Gomes, C. B. (1981). Alkaline rocks from continental Brazil. *Tectonophysics* **17,** 135–154.

Ussami, N. & Molina, E. C. (1997). Geoid anomalies of the Parana province: new constraints on density distribution and thermal state of the lithosphere. *Eos Transactions, American Geophysical Union* **78,** 748.

Valença, J. G. & Edgar, A. D. (1979). Pseudoleucites from Rio de Janeiro State, Brazil. *American Mineralogist* **64,** 733–735.

Valente, S. C., Meighan, I. G., Fallick, A. E. & Ellam, R. L. (1995). Os diques de rochas alcalinas do Rio de Janeiro, RJ. *V Congresso Brasileiro de Geoqutímica*, Niterói/RJ. (No page numbers. This publication is only available as a CD-ROM from Sociedade Brasileira de Geoquímica, Rio de Janeiro.)

VanDecar, J. C., James, D. E. & Assumpção, M. (1995). Seismic evidence for a fossil mantle plume beneath South America and implications for plate driving forces. *Nature* **378,** 2531.

Waber, N., Schorscher, H. D. & Peters, T. (1992). Hydrothermal and supergene uranium mineralisation at the Osamu Utsumi mine, Poços de Caldas, Minas Gerais, Brazil. *Journal of Geochemical Exploration* **45,** 53–112.

Watson, S. & McKenzie, D. (1991). Melt generation by plumes: a study of Hawaiian volcanism. *Journal of Petrology* **32,** 501–537.

White, R. S. & McKenzie, D. (1995). Mantle plumes and flood basalts. *Journal of Geophysical Research* **100,** 17543–17585.

Wilkinson, P., Mitchell, J. G., Cattermole, P. J. & Downie, C. (1986). Volcanic chronology of the Meru–Kilimanjaro region, northern Tanzania. *Journal of the Geological Society, London* **143**, 601–605.

Woolley, A. R. (1987). *Alkaline Rocks and Carbonatites of the World: Part 1: North and South America*. London: British Museum (Natural History), 216 pp.

Woolley, A. R., Bergman, S. C., Edgar, A. D., Le Bas, M. J., Mitchell, R. H., Rock, N. M. & Scott Smith, B. (1996). Classification of lamprophyres, lamproites, kimberlites, and the kalsilitic, melilitic and leucitic rocks *Canadian Mineralogist* **34,** 175–186.

Wyllie, P. J. (1988). Solidus curves, mantle plumes and magma generation beneath Hawaii. *Journal of Geophysical Research* **93,** 4171–4181.

APPENDIX A: SAMPLE LOCALITIES

NOTE: Samples collected in 1994 (prefix 94) have localities that include GPS positions (WGS84 datum).

90SB64, 67, 68: Road between Cascata and Águas de Prata, Poços de Caldas. Post 245 km from São Paulo.

90SB70, 72: Same section as above. Post 246 km.

90SB75, 79: Same section as above. Post 249 km.

93SOB198, 205, 206: Ponte Nova complex, near Campos do Jordão. Route 42, from Sapucaí Mirim to Santo Antônio do Pinhal.

93SOB208, 209, 210: 4 km south of Campos do Jordão, on road to Santo Antônio do Pinhal.

93SOB212: Road between Sapucaí Mirim and Bairro São José.

93SOB213: Steepest section of road from Santo Antônio do Pinhal to Pico Agudo.

94SOB90, 91, 92: Quarry in basement gneiss, Passa Quatro (22°26′52″S, 44°44′09″W).

94SOB95: Road between Moringa and Cachoeira, Itatiaia complex (20°18′22″S, 44°33′24″W).

94SOB97, 98: Escarpment above Resende, Itatiaia complex (22°21′01″S, 44°30′35″W).

94SOB57, 58, 61, 64: Sentíssimo quarry, Campo Grande, near Rio de Janeiro (22°53′00″S, 43°29′27″W).

94SOB66, 67: Bangu quarry, Rio de Janeiro (22°53′17″S, 43°27′32″W).

94SOB68: Realengo quarry, Rio de Janeiro (22°53′13″S, 43°24′18″W).

94SOB78, 80, 81: Nova Iguaçu quarry, Rio de Janeiro (22°46′11″S, 43°29′45″W).

94SOB50, 51: Disused quarry, São José do Itaboraí (22°50′25″S, 42°52′46″W).

94SOB127, 128, 131: Stream draining Serra do Bertholdo, NW of Soarinho (22°34′01″S, 42°39′27″W).

94SOB142: Fazenda Ventania, Morro de São João (22°30′59″S, 42°01′49″W).

93SOB191: Ponta do Boqueirão, Cabo Frio.

93SOB193: Ponta Prainha, Cabo Frio.

93SOB196, 197: Pontal do Atalaia, Cabo Frio.

94SOB14, 17: Trigo island (23°51′32″S, 45°46′27″W).

94SOB20: Trigo island (23°51′44″S, 45°46′31″W).

94SOB10, 12, 13: Eastern side of Praia Preta, São Sebastião (23°49′17″S, 45°24′34″W).

90SB54: Praia do Aramasola, Ilhabela.

94SOB31: Praia do Curral, Ilhabela (23°51′34″S, 45°25′05″W).

94SOB55: Roadside, Estrada do Grumari (23°03′04″S, 43°32′51″W).

94SOB56: Roadside, Fazenda Modelo (22°59′49″S, 43°35′30″W).

94SOB89: Roadside, 4·5 km SE of Volta Redonda (22°32′13″S, 44°04′35″W).

APPENDIX B: ICP-MS TECHNIQUES

Powders were dissolved using a standard HF–HNO_3 technique, with care being taken to ensure no fluoride residue. Samples were spiked with Rh, In and Bi, to monitor internal drift, before dilution to 3·5% HNO_3. The resulting solutions were analysed on a Perkin–Elmer SCIEX Elan 6000 inductively coupled plasma mass spectrometer, using a cross-flow nebulizer. Oxide interferences for most analytes were <3% of the total signal; appropriate corrections were made using oxide/metal ratios, measured on matrix-matched standard solutions. Calibration was achieved using matrix-matched international rock standards plus in-house standards. Total procedural blanks for all elements were negligible for all analytes. Reproducibility, based on replicate digestions of standards and samples, varied from 1·5% to 3% for most analytes.